University of Massachusetts Amherst

ScholarWorks@UMass Amherst

LmeA, a Conserved Cell-Envelope Protein in Mycobacteria, is Important for Antibiotic Resistance and Cell Envelope Permeability

Sarah Hassan Osman
University of Massachusetts Amherst

Follow this and additional works at: https://scholarworks.umass.edu/masters_theses_2

Part of the Bacteriology Commons, and the Biochemistry Commons

Recommended Citation

LmeA, a Conserved Cell-Envelope Protein in Mycobacteria, is Important for

Antibiotic Resistance and Cell Envelope Permeability

A Thesis Presented

By

SARAH HASSAN OSMAN

Submitted to the Graduate School of the

University of Massachusetts Amherst in partial fulfillment

of the requirements for the degree of

MASTER OF SCIENCE

May 2020

Microbiology

LmeA, a Conserved Cell-Envelope Protein in Mycobacteria, is Important for

Antibiotic Resistance and Cell Envelope Permeability

A Thesis Presented

By

SARAH HASSAN OSMAN

Approved as to style and content by:

DocuSigned by:

Yasu S. Morita

7FB831114FBC40C...

Yasu S. Morita, Chair

DocuSigned by:

M. Sloan Siegrist

2FF909704E16447...

Sloan S. Siegrist, Member

DocuSigned by:

Wilmore C. Webley

6FAF3DE528EF4E9...

Wilmore C. Webley, Member

DocuSigned by:

1F0CE8945AD74BE...

James F. Holden, Department Head

Microbiology

DEDICATION

To my parents, who came to this country in search of opportunity, and who have always

prioritized the education of their children.

ACKNOWLEDGEMENTS

ABSTRACT

LMEA, A CONSERVED CELL-ENVELOPE PROTEIN IN MYCOBACTERIA, IS IMPORTANT FOR ANTIBIOTIC RESISTANCE AND CELL ENVELOPE PERMEABILITY

MAY 2020

SARAH HASSAN OSMAN

B.S. UNIVERSITY OF MASSCHUSETTS AMHERST

M.S. UNIVERSITY OF MASSCHUSETTS AMHERST

Directed by: Professor Yasu S. Morita

The cell envelope of mycobacteria is critical for the survival and virulence of pathogenic species during infection, and its biosynthesis has been a proven drug target. Therefore, finding new targets in the biosynthetic pathway of cell envelope components is of great interest. *Mycobacterium smegmatis* is a model organism for the study of the devastating pathogen *Mycobacterium tuberculosis*. Previously, lipomannan elongation factor A (LmeA) has been identified as a cell envelope protein that is critical for the control of mannan chain length of lipomannan (LM) and lipoarabinomannan (LAM), lipoglycan components of the cell envelope. The deletion mutant, Δ*lmeA*, accumulates abnormal LM/LAM with fewer mannan residues. To understand the importance of this protein, the antibiotic sensitivity of Δ*lmeA* was tested using a

resazurin-based viability assay. We found that the *lmeA* deletion leads to increased sensitivities to antibiotics such as vancomycin and erythromycin, and *lmeA* overexpression leads to increased antibiotic resistance. To directly test if the increased antibiotic sensitivity is due to the defective permeability barrier, we used an ethidium bromide uptake assay and found that Δ*lmeA* is more efficient in taking up ethidium bromide in the cell. We have also found that LmeA is important for protein stabilization under stress conditions. MptA is an α1,6-mannosyltransferase involved in elongation of LM and LAM mannan chain. During stress conditions in the *ΔlmeA* mutant, levels of MptA decrease significantly relative to wild-type. This also results in delayed doubling time after stress, a phenotype not seen in this mutant under normal growth conditions. In addition, the *ΔlmeA* mutant has differential protein expression during stress conditions relative to *ΔlmeA* in log phase, or to wild-type in either condition. To help elucidate the role of LmeA at the molecular level, binding behavior of this protein to membrane fractions was determined. In a subcellular fractionation analysis, LmeA localizes to fractions containing plasma membrane, which is tightly bound to cell wall layers. To test the binding of LmeA to membrane further, LmeA was heterologously expressed in *Escherichia coli*, purified, and mixed *M.* smegmatis cell lysate. LmeA localized to intracellular domain fractions (IMD), indicating that LmeA is capable of localizing to fractions containing only plasma membrane. Consistent with this finding, LmeA is capable of binding to spheroplasts in both an ELISA setting as well as in a sucrose gradient fractionation setting. It has also been determined that *ΔlmeA* has a defective capsular layer with a unique phenotype relative to other strains. We have concluded that LmeA is important for antibiotic resistance, cell envelope permeability, capsule formation, stress response, and have also determined its binding properties.

TABLE OF CONTENTS

LIST OF TABLES

LIST OF FIGURES

Chapter 1
Introduction

1.1 Medical relevance

Mycobacteria are a medically relevant genus of bacteria. In particular, *Mycobacterium tuberculosis* (*M. tb*), the human pathogen and main causative agent of tuberculosis, is of global concern. *M. tb* has played a large role throughout history, wiping out large portions of societies and shaping disease surveillance. The earliest evidence of *M. tb* infections has been found in human remains going back as far as 5000 BCE in Peru and Egypt [1]. The earliest documents found describing tuberculosis date back 3,300 years ago in India[2]. Later, between the 1600s and 1800s, tuberculosis accounted for one quarter of all deaths in Europe[3]. Although there have been great public health and medical advances, tuberculosis is a health issue countries continue to battle globally. It is estimated that about one-quarter of the current global population is infected with *M. tb*[4] . Of this group, between 5 and 15 percent will go on to develop active tuberculosis with the remaining percentage having dormant, non-infectious, and non-disease-causing *M. tb* infections[5] . These numbers translate into 10 million new, active cases each year and 1.5 million deaths[4] . The majority active *M. tb* infections occur in low- and middle-income countries, but the disease is still widespread. For example, in the United States, 8,920 cases of active tuberculosis were reported, with an estimated 13 million latent infections[5] . The treatment of tuberculosis is multi-pronged and lengthy, requiring the use of many drugs over a long period of time. Standard treatment for non-drug resistance tuberculosis in non-HIV patients consists of a two-month intensive phase of isoniazid, rifampin, pyrazinamide, and ethambutol followed by a four-month phase of isoniazid and rifampicin[6]. Despite the global research effort and the many advancements in understanding this pathogen, the discovery of new drugs for tuberculosis treatment has stalled, with only one new drug meeting FDA approval in the past 40 years[7]. This

is especially concerning due to the rise in multidrug-resistance and extensively drug-resistant tuberculosis infections[8].

1.2 Cell Envelope Overview

A large part of what makes *M. tb* such a good pathogen is its complex and waxy cell envelope. This multilayered barrier protects the cell from threats like antibiotics and host defenses and can even modulate the human immune system[9]. In addition to providing protection to the cell, the cell envelope is necessary to provide the rigidity and shape to these rod-shaped microbes. The mycobacterial cell envelope is composed of several layers. The innermost layer begins with the plasma membrane, a phospholipid bilayer. This plasma membrane is composed of different lipids such as cardiolipin, phosphatidylethanolamine, phosphatidylinositol, phosphatidylinositol mannosides (PIMs), and menaquinones, as well as others. Furthermore, mycobacterial compartmentalize plasma membrane. In *Mycobacterium smegmatis*, the non-pathogenic and fast-growing model organism for *M. tb*, a lipid domain coined intracellular membrane domain (IMD) is spatially distinct from the rest of the plasma membrane[10]. The IMD contains unique metabolic enzymes often involved in cell envelope biosynthesis, and these proteins tend to localize to the polar regions of the cell. The IMD is also dynamic, responding to environmental stresses such as starvation[11]. The next layer is a thick peptidoglycan core, on par with other gram-positive bacteria, with the periplasmic space residing underneath. This mesh of sugars and amino acids allows the cell to maintain its shape and rigidity[12]. When this peptidoglycan layer is removed and digested by lysozyme, the cell changes shape and eventually lyses. Moving upwards is the arabinogalactan layer. This layer is composed of galactose and arabinose polymers and is covalently bound to the outer membrane above it, also known as the

mycomembrane. The outer membrane is heavy in mycolic acids and abundant in glycans and lipids like lipomannan and lipoarabinomannan, glycolipids with great significance in immune modulations[13]. This membrane forms a sort of bilayer lipidic membrane, similar in structure to the plasma membrane. Current research suggests that the inner leaflet of this layer is mostly formed of mycolic acids while the outer leaflet of different lipidic species like trehalolipids and possibly lipomannan and lipoarabinomannan[14]. These mycolic acids covalently link this layer to the arabinogalactan layer. Finally, there is the capsule, the outermost layer made of polysaccharides that directly interacts with the environment surrounding the microbe. The capsular layer plays a role in variety of processes such as the formation of biofilms and host immunity resistance[15]. This layer is non-covalently attached and can be visualized by electron microscopy. The mycobacterial capsule is composed of uncharged polysaccharides such as α-glucan, arabinomannan, and mannan. The capsule can be visualized by the mannan and glucan binding fluorescent-conjugated lectin, Concanavalin A. The capsule plays a role in host immune response, with host receptors recognizing α-glucan[16] .
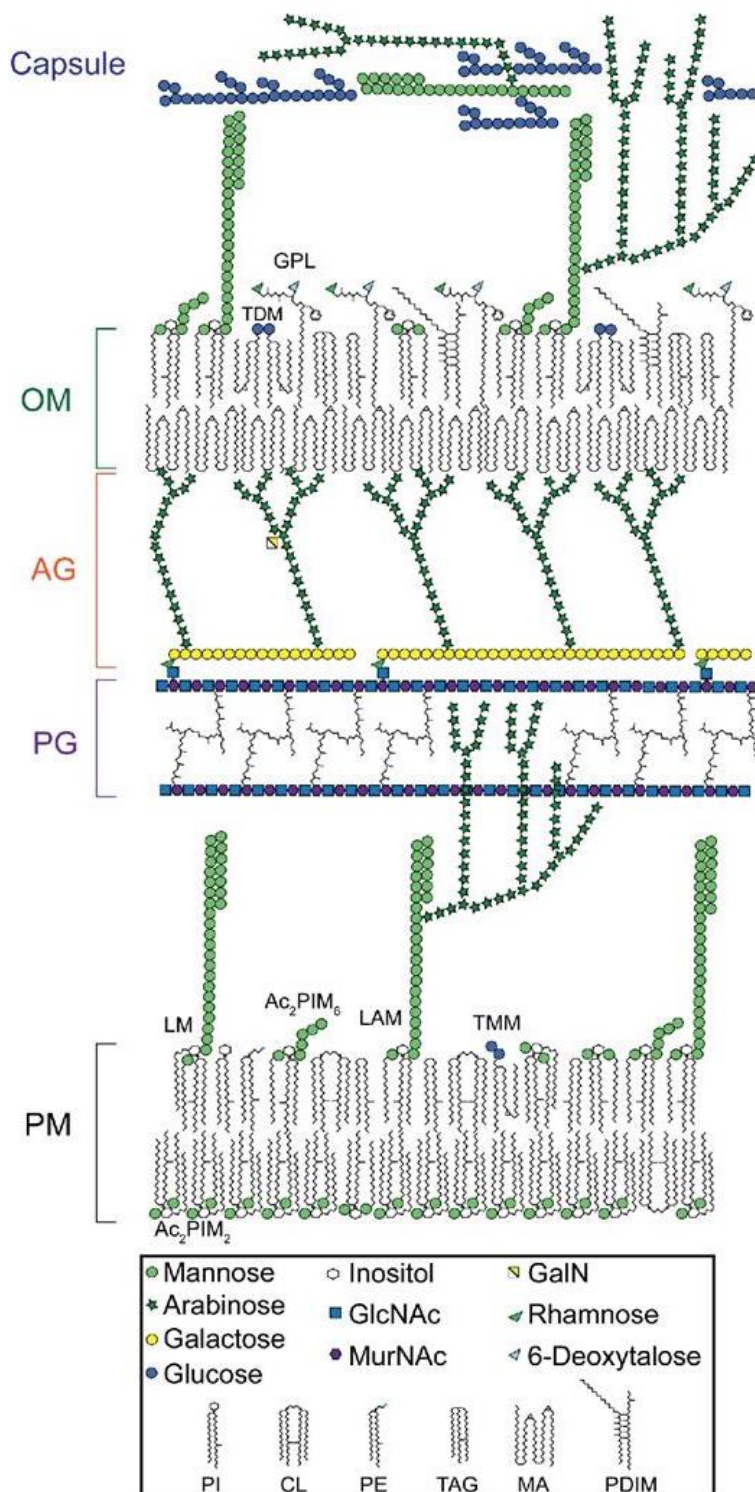
Figure 1.1: The Mycobacterial Cell Envelope Figure taken from *Pathogens and Disease*, Volume 76, Issue 4, June 2018[10]. The mycobacterial cell envelope begins with the plasma membrane. The periplasmic space sits between the plasma membrane and the peptidoglycan core. Moving upwards, an arabinogalactan layer is followed by the outer membrane. The outermost layer is the capsule.

1.3 Biosynthesis of Cell Envelope Components

The biosynthesis of different components and layers of the mycobacterial cell envelope is a complex process involving the use of many different enzymes and other proteins. Of relevance to this study is the biosynthesis of phosphatidylinositol mannosides, lipomannan, and lipoarabinomannan, major components of the plasma membrane.

The most abundant PIM species in *M. smegmatis*, the model organism for *M. tb*, are AcPIM2 and AcPIM6. Production of these PIMs begin with the synthesis of phosphatidylinositol (PI) from inositol and cytidine diphosphate diacylglycerol (CDP-DAG). This reaction requires no energy input and is controlled by the PI synthase PgsA, which has been found to be essential in *M. smegmatis* [17]. From there, PI can be decorated with varying numbers of mannose residues and fatty acid modifications. In the case of AcPIM2, PI has two mannose residues added sequentially by PimA and PimB' respectively [18]. An acyl chain is then added to one of the mannose residues by PatA [19]. The enzymes responsible for the first two mannose additions, PimA and PimB', mostly likely operate on the cytoplasmic side of the plasma membrane, as suggested by the fact that they are GDP-mannose-dependent enzymes. The formation of AcPIM6 is less clear. The mannosyltransferase(s) that form AcPIM4 from AcPIM2 is still unknown in mycobacteria. After AcPIM4 is formed, a mannosyltransferase termed PimE drives the production of AcPIM6 by adding a fifth mannose to AcPIM4 using polyprenol-phosphate-mannose (PPM) as a mannose donor [20].

Lipomannan (LM) and lipoarabinomannan (LAM) biosynthesis begins with AcPIM4. A lipoprotein termed LpqW has been shown to be involved in the branching point of AcPIM4 to either AcPIM6 or LM/LAM [21]. The mannan chain of AcPIM4 is elongated to 5-20 residues to form an LM intermediate. MptA, another mannosyltransferase, elongates this α1,6 mannan chain

to 21-34 residues[22] . The protein of focus in this study, LM elongation factor A (LmeA), is necessary for the α1,6 mannan elongation by MptA. The mannosyltransferase MptC decorates the α1,6 mannan backbone by α1,2 mono-mannose chains.[23] To form LAM, one arabinan residue is attached to the mannan backbone. The first arabinosyltransferase is still unknown but EmbC, an α1,3 araibonsyltransferase, elongates the primed arabinose[24] . AftC and AftB are also involved in this arabinan addition as well as arabinogalactan biosynthesis[25,26] .
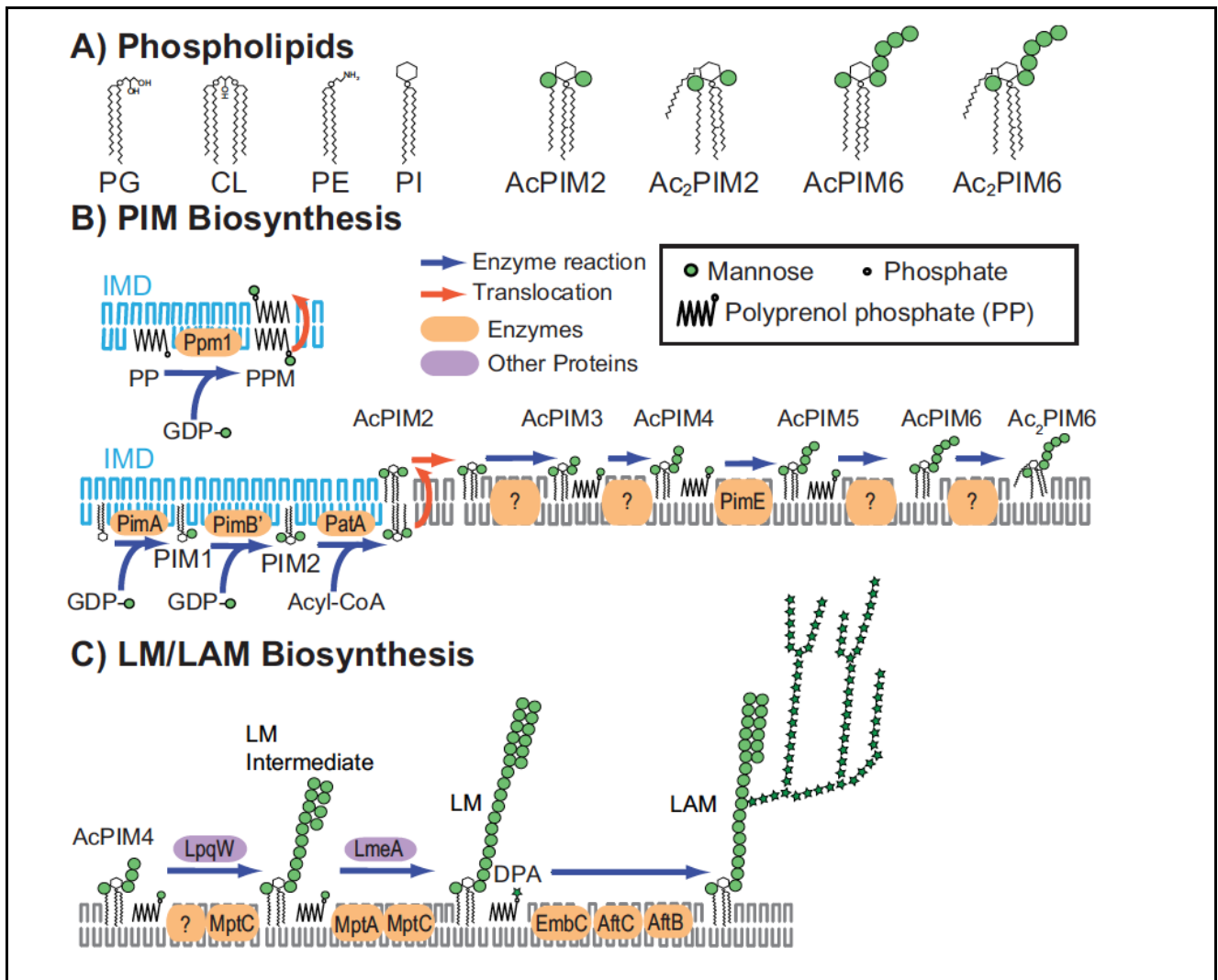
Figure 1.2: Biosynthesis of Phospholipids, PIMs, and LM/LAM. Figure by Kathryn Rahlwes [27].

1.4 Intracellular Membrane Domain

A lipid domain coined intracellular membrane domain (IMD) has been characterized in *M. smegmatis*[17]. This is a dynamic but spatially distinct part of the plasma membrane in mycobacteria which contains cell envelope biosynthetic reactions. Mycobacteria grow in a polar manner, suggesting that there may be spatiotemporal control mechanisms to provide cell envelope precursors to this area. Microscopy has shown that IMD proteins tend to localize and be enriched in the polar regions of the cell. The IMD, or plasma membrane free of cell wall components, is biochemically separate from plasma membrane components that are bound to cell wall fractions (PMCW). In a sucrose gradient fractionation, IMD proteins go to unique fractions, separate from cytoplasmic and PMCW proteins. Proteomic analysis has shown that these IMD fractions enzymes related to the biosynthesis of PIMs, suggesting it plays a major role in PIM metabolism. The IMD is dynamic and responsive to environmental stresses[11]. The IMD localizes specifically to the polar region where active growth is taking place. The IMD also repositions from the poles to the sidewall during starvation or other stress conditions[11] .

1.5 Spheroplasts

As previously mentioned, the mycobacterial membrane is complex and multilayered. Spheroplasts have the mycomembrane and cell wall layers stripped off. In order to do this, glycine is added to inhibit the biosynthesis of peptidoglycan[28]. Then, lysozyme is added to remove any existing peptidoglycan. As the peptidoglycan is removed, all the layers above it are also removed. Without this peptidoglycan exoskeleton, the resulting wall-deficient cell transitions from a rod to a sphere. Spheroplasts are especially fragile, requiring the use of osmotic protective media in order to keep these cells from lysing. Studies have shown that only

the lipidic anchors of LM and LAM are left the cell envelope after spheroplasting[29] . This form

of mycobacterial cells can be especially useful in characterizing plasma membrane associated

proteins.

1.6 *M. smegmatis*'s Relevance to *M. tuberculosis*

M. tb and *M. smegmatis* are species of bacteria within the class of actinobacteria. They

are gram-positive, rod shaped cells that grow by inserting new cell envelope material at the

poles. A defining feature of these mycobacteria are the high GC content, with *M. tb* measuring at

65.6% and *M. smeg*matis measuring at 67.4% [30]. Another defining feature of these species are

their complex and multilayered cell envelope, of which the two are highly similar. *M. smegmatis*

is often used as the model organism to study *M. tb* and other pathogenic mycobacteria due to its

non-pathogenicity and fast doubling time. *M. smegmatis* doubles every 3-4 hours while *M.*

tuberculosis doubles every 24 hours. *M. smegmatis* shares high genome identity with *M.*

tuberculosis, making it a good model for study[31]. This study will use *M. smegmatis* as a model,

and all proteins mentioned in the results section have been confirmed to have homologs in *M.*

tuberculosis.

1.7 Previous Data and Aims of this Study

The biosynthesis of cell envelope components is a proven target in treating *M.*

tuberculosis infections. Ethambutol, one of the few drugs approved to treat tuberculosis, inhibits

the enzyme that polymerizes arabinose into arabinogalactan[32]. Isoniazid, another drug used for

treatment, inhibits the synthesis of mycolic acids[33]. Therefore, it is reasonable to expect that the

next approved drug may target a protein involved in cell envelope biosynthesis, so understanding these pathways is of importance.

Previously, it has been shown that the deletion of the *pimE* gene, which encodes the enzyme responsible for the committed step in AcPIM6 formation, results in a small colony morphology[34]. This small colony morphology was used to identify suppressor mutants of Δ*pimE*, some of which had significantly shorter LM and LAM. After genome sequencing, it was shown that some of these suppressor mutants had a mutation in *MSMEG_5785*, or *lmeA*. Subsequent testing showed that LmeA is a PMCW protein and Δ*lmeA* results in short LM and LAM, but not a change in colony size or doubling time[35]. It was also found that in Δ*lmeA* under stress conditions, MptA degradation occurs (Rahlwes KC, unpublished observations). Lastly, it was shown that LmeA binds to phospholipids[35]. These previous data provide clues to LmeA's role, but its exact function is still unclear. This study further elucidated LmeA's role in cell envelope biosynthesis and includes the following chapters:

I. **Chapter 2: Impact of LmeA on Cell Envelope Integrity and Homeostasis:** This aim includes antibiotic sensitivity, cell envelope permeability, protein expression under log and starvation conditions, and capsule staining.

II. **Chapter 3: LmeA Localization and Cell-Envelope Binding Properties:** This aim includes LmeA binding *in-vivo*, *in-vitro*, and to spheroplasts.

III. **Chapter 4: LmeA's Role in MptA Stabilization and Possible Interactions with ThiX:** This chapter includes the characterization of Δ*lmeA* under stress conditions and the investigation of the relevance of ThiX, a protein encoded by a gene in the same operon as *LmeA*.

Chapter 2
Impact of LmeA on Cell Envelope Integrity and Homeostasis

2.1 Previous Data Within This Aim

lmeA was first identified by finding suppressor mutants of Δ*pimE*. *pimE* encodes the first

committed step in phosphatidylinositol hexomannoside biosynthesis in *M. smegmatis* and a

knockout mutant of this gene results in a small colony morphology. This small colony morphology

was used to find suppressor mutants that restored the wild-type colony size morphology. Of the

suppressor mutants that were found, three suppressor mutants termed S1, S10, and S22 had

mutations in *MSMEG_5785*. This gene was later termed *lmeA*. These suppressor mutants were

able to restore colony size but had smaller LM and LAM. Complementation of *lmeA* to these

Δ*pimE* mutants with non-functional LmeA were able to restore LM and LAM back to the WT

phenotype. Δ*lmeA* also showed a small LM and LAM phenotype[35].

2.2 Antibiotic Sensitivity

LmeA has been predicted to be essential in *M. tb* and a previous study has shown that

LmeA is upregulated during mouse infection[36]. It has been shown that when mycobacterial cells

have short LM and LAM, antibiotic sensitivity increases[37]. These facts taken together with the

short LM and LAM in the Δ*lmeA* mutant led us to investigate LmeA's role in cell envelope

integrity in terms of antibiotic sensitivity. Antibiotic sensitivity was determined through a

resazurin-based assay. Resazurin is a colorimetric dye that can be used for viability dose-

response assays. As cells grow and produce reduced electron carriers, these reduced electron

carriers can reduce resazurin, which is blue, to resorufin, which is pink. The 96-well plate can

then be read at the appropriate wavelengths, and the output is run through an equation that

translates the wavelengths into percent growth relative to a positive control. The percent growth

is then graphed and the inhibitory concentration that inhibits 90% of growth (IC90) is calculated, which is what is listed below in Table 1. All values were done in triplicate.
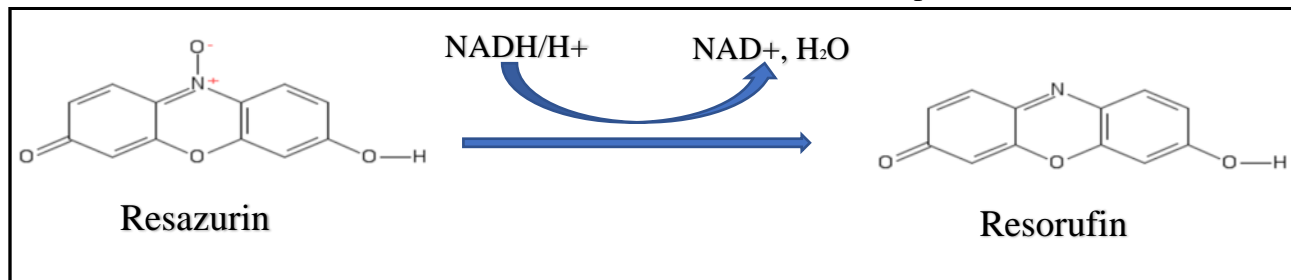
Figure 2.1: The Reduction of Resazurin As cells grows and produce reduced electron carriers like NADH, these reduced electron carriers reduce resazurin (blue) to resorufin (pink).

	Vancomycin	Cefotaxime	Ampicillin	Clarithromycin	Erythromycin
WT	1.00 +/- 0.14	>100	>100	0.15 +/- 0.01	0.96 +/- 0.17
$\Delta lmeA$	0.39 +/- 0.04	9.77 +/- 2.08	70.04 +/- 14.77	0.05 +/- 0.01	0.12 +/- 0.01
$\Delta lmeA$::P$_{native}$-$lmeA$-HA	0.58 +/- 0.09	48.23 +/- 7.56	>100	0.15 +/- 0.01	0.31 +/- 0.01
$\Delta lmeA$::P$_{hsp60}$-$lmeA$-HA	1.90 +/- 0.29	>100	>100	0.65 +/- 0.18	2.30 +/- 0.79
WT::P$_{hsp60}$-$lmeA$-HA	1.73 +/- 0.41	>100	>100	0.71 +/- 0.38	5.85 +/- 0.9
WT::P$_{hsp60}$-$lmeA$-HA (Episomal)	2.13 +/- 0.33	>100	>100	0.25 +/- 0.05	0.92 +/- 0.21
$\Delta pimE$	0.24 +/- 0.01	84.41 +/- 3.78	>100	0.09 +/- 0.01	0.49 +/- 0.08
S10	0.23 +/- 0.01	10.13 +/- 1.35	64.1 +/- 6.27	0.09 +/- 0.02	0.19 +/- 0.01
S10::P$_{hsp60}$-$lmeA$-HA	0.31 +/- 0.01	>100	>100	0.89 +/- 0.2	10.55 +/- 3.41
S22	0.19 +/- 0.01	9.05 +/- 1.24	45.09 +/- 1.43	0.05 +/- 0.01	0.09 +/- 0.02

Table 2.1 Antibiotic susceptibility of various strains. IC90 values of various strains treated with a range of antibiotics at 37°C. Units in µg/ml. Green indicates increased antibiotic resistance relative to wildtype. Red indicates increased antibiotic sensitivity relative to WT.

Treating *M. tb* infections requires the use of different classes of antibiotics with some targeting the cell envelope and others having cytoplasmic targets. For this reason, it was of interest to test a range of antibiotics. Vancomycin is a large antibiotic that binds to N-acetylmuramic acid and N-acetylglucosamine, the building blocks of peptidoglycan, to inhibit the crosslinking of this layer[38]. Cefotaxime and ampicillin are beta-lactams that inhibit cell wall synthesis by binding to penicillin-binding proteins[39]. Cells with defective cell envelopes should show increased sensitivity to these antibiotics. Clarithromycin and erythromycin are small antibiotics with cytoplasmic targets. These two antibiotics are macrolides that bind to the 23S ribosomal RNA of the 50S subunit of the ribosome, inhibiting the transpeptidation and translocation step of protein synthesis[40] .

ΔlmeA is more sensitive to all antibiotics tested relative to WT. When *lmeA* is complemented back with a native promoter to this knockout mutant, antibiotic sensitivity decreases. This complement is able to restore antibiotic resistance in the case of ampicillin and clarithromycin but does not fully restore in the case of vancomycin, cefotaxime, and erythromycin. When the ΔlmeA mutant is complemented with a heat shock protein 60 promoter granting constitutive expression, *lmeA* is expressed at a higher level than the native promoter, and antibiotic resistance increases. Antibiotic resistance is completely restored in the case of cefotaxime and ampicillin. This strain becomes even more resistant to antibiotics relative to WT in the case of vancomycin, clarithromycin, and erythromycin. When *lmeA* is expressed from the HSP60 promoter in a WT background, similarly increased levels of antibiotic resistance was observed. The strain remains resistant to cefotaxime and ampicillin, and becomes more resistant to vancomycin, clarithromycin, and erythromycin relative to WT. In the next strain, *lmeA* expressed was increased by expressing *lmeA* episomally using the heat shock protein 60

promoter in the WT background. The strain showed the highest resistance to vancomycin, maintained resistance to beta-lactams and erythromycin, and showed increased resistance to clarithromycin. Taken together, this data shows that the absence of LmeA leads to an increase in sensitivity to a range of antibiotics and the complementation and overexpression of LmeA leads to antibiotic resistance.

Because *lmeA* was identified through finding suppressor mutants of Δ*pimE*, it was of interest to investigate how antibiotic sensitivity compares between Δ*lmeA*, Δ*pimE*, and the suppressor mutants. Both deletion mutants show an increase in antibiotic susceptibility but Δ*pimE* is slightly more resistant to antibiotics compared to Δ*lmeA*, except in the case of vancomycin. Interestingly, in the case of the suppressor mutants S10 and S22 which are missing a *pimE* deletion and have non-functional LmeA, antibiotic sensitivity did not significantly increase relative to either of the single knockout mutants. Complementation of *lmeA* back into the S10 suppressor mutant did improve antibiotic sensitivity, even resulting in the highest antibiotic resistance for clarithromycin and erythromycin.

Another avenue that was investigated in terms of antibiotic sensitivity was the effect of temperature. The previous antibiotic sensitivity table was done at 30°C. It was of interest to determine if increasing the temperature to 37°C, the temperature of the human body, would have a differential effect on WT relative to Δ*lmeA*. The tables below show the results.

Temp. (°C)		Vancomycin	Cefotaxime	Ampicillin	Clarithromycin	Erythromycin
30	WT	1.51 +/- 0.26	>100	>100	0.49 +/- 0.09	3.52 +/- 1.08
	ΔlmeA	1.00 +/- 0.11	>100	>100	0.14 +/- 0.01	0.82 +/- 1.03
	ΔlmeA::Pnative-lmeA-HA	0.37 +/- 0.04	>100	>100	0.05 +/- 0.01	0.25 +/- 0.05
37	WT	1.00 +/- 0.14	>100	>100	0.15 +/- 0.01	0.96 +/- 0.17
	ΔlmeA	0.39 +/- 0.04	9.77 +/- 2.08	70.04 +/- 14.77	0.05 +/- 0.01	0.12 +/- 0.01
	ΔlmeA::Pnative-lmeA-HA	0.58 +/- 0.09	48.23 +/- 7.56	>100	0.15 +/- 0.01	0.31 +/- 0.01

Table 2.2: IC90s of Various Strains in 7H9 Media at 30°C vs 37°C IC90s in the presence of various antibiotics. Units are in µg/ml.

It is known that as the temperature increases, the fatty acid tails of phospholipids in the plasma membrane become less rigid, and this can lead to increased membrane fluidity. This corresponds to the general trend when looking at the above Table 2.2 When the temperature was increased to 37°C, WT and Δ*lmeA* became more sensitive to antibiotics. WT maintained its resistance to beta-lactams regardless of the temperature change. In the case of vancomycin, cefotaxime, ampicillin, and erythromycin, Δ*lmeA*'s percent change in IC90 from 30°C to 37°C was higher than WT's. As seen before, this native promoter complement was unable to fully restore antibiotic sensitivity. At 37°C, the complement partially recovers antibiotic resistance. At 30°C, the complement is unable to restore antibiotic resistance.

In a previous publication, I determined the antibiotic sensitivity for WT in M63 media[34]. Later, for another project, I looked at antibiotic sensitivity in M63 media but this time leaving out Tween-80, the detergent typically used in mycobacterial cultures to mimic biofilm conditions. Table 2.3 demonstrates that adding and removing tween can drastically change antibiotic sensitivity in WT.

	Vancomycin	Cefotaxime	Ampicillin	Clarithromycin	Erythromycin
M63 – Tween	>100	>100	>100	1.61 +/- 0.24	78.87 +/- 28.23
M63 + Tween	15.03 +/- 3.99	>100	>100	>100	>100

Table 2.3: IC90s of Wildtype in M63 Media in the Presence and Absence of Tween-80 IC90 values of wildtype treated with a range of antibiotics at 37°C. Units in µg/ml.

Following the confirmation of the effects of Tween-80 on the antibiotic susceptibility of wild type, the next step was to see if this trend held true for Δ*lmeA*. Below in Table 2.4 are the results.

	7H9-Tween	7H9 + Tween
WT	8	1.00 +/- 0.14
Δ*lmeA*	0.4	0.39 +/- 0.04

Table 2.4: Vancomycin IC90s of WT and Δ*lmeA* in the Presence and Absence of Tween-80 in 7H9 Media at 37°C. Units in µg/ml.

Using 7H9 media, tween was either added or removed and the IC90 of WT and Δ*lmeA* was determined. Without tween, antibiotic resistance increases in WT. Interestingly, the presence of tween does not make a different in IC90 in Δ*lmeA* as it does in WT. Tween interacts with the outside-most layer of the cell envelope- the capsule. This led us to believe that perhaps Δ*lmeA* already has a defective capsule, and so the addition tween makes no difference.

Another interesting pattern seen in Table 2.4 was that M63 was able to increase antibiotic resistance. The last of the antibiotic sensitivity tests was to see if M63 can increase antibiotic resistance in Δ*lmeA* in the same manner it does in WT.

	Vancomycin	Cefotaxime	Ampicillin	Clarithromycin	Erythromycin
WT	>100	>100	>100	1.61 +/- 0.24	78.87 +/- 28.23
ΔlmeA	14.70 +/- 2.92	>100	>100	0.35 +/- 0.03	0.41 +/- 0.16
ΔlmeA::P$_{native}$-lmeA-HA	99.60 +/- 17.89	>100	>100	0.61 +/- 0.02	9.51 +/- 1.64

Table 2.5: IC90s of Various Strains in M63 Media IC90 values of various strains treated with a range of antibiotics at 37°C. Units in µg/ml.

Indeed, Δ*lmeA* was able to show increased resistance to antibiotics across the board when grown in M63 media without tween at 37°C. WT became completely resistant to vancomycin, maintained resistance to the beta-lactams, and showed increased resistance to macrolides, erythromycin in particular. Δ*lmeA* became more resistant to antibiotics across the board as well, becoming completely resistant to beta-lactams.

2.3 Cell Envelope Permeability

As shown in the previous section, Δ*lmeA* showed increased antibiotic sensitivity to a range of different antibiotics relative to WT. The next step in confirming this mutant's defective cell envelope was to examine cell envelope permeability. Cell envelope permeability was determined through an ethidium bromide uptake assay. Ethidium bromide binds DNA located inside of the cell. If the cell envelope is more permeable, more ethidium bromide will bind to DNA and fluoresce. Fluorescence excitation at 530 nanometers and the resulting emission at 590 nanometers was measured over a time course and plotted.
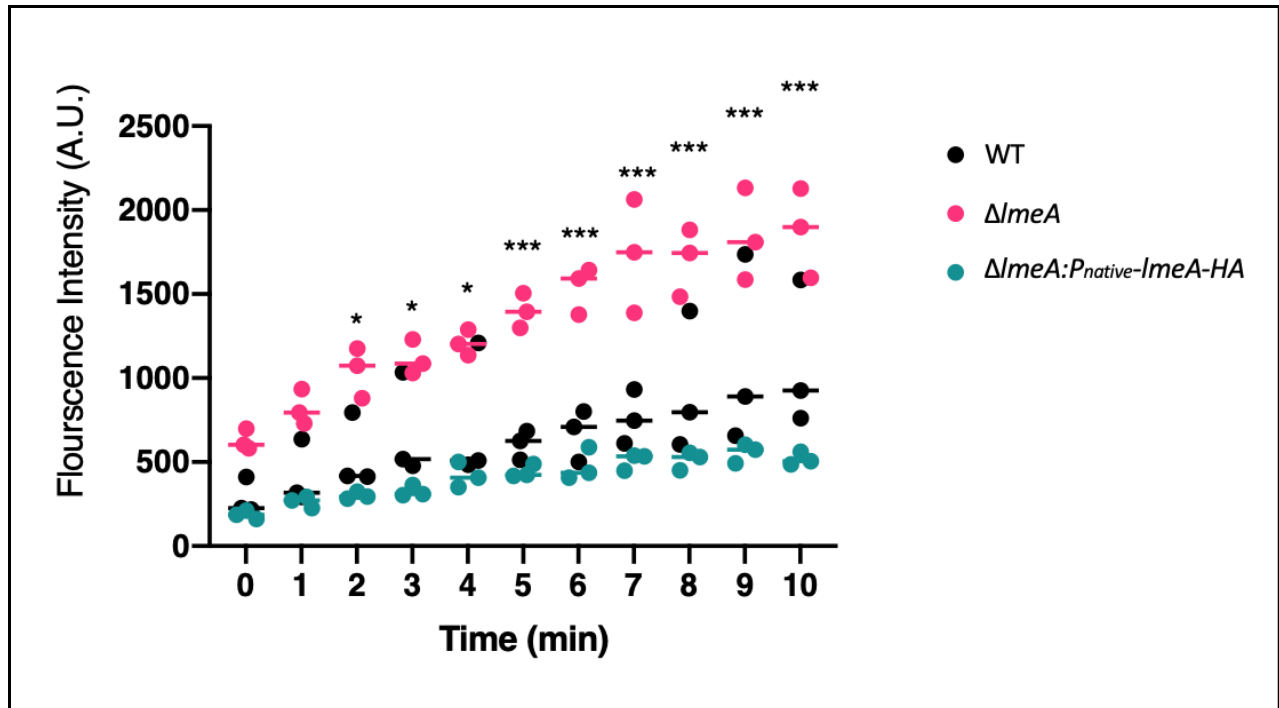
Figure 2.2: Ethidium Bromide Permeability Assay 20 µM ethidium bromide uptake assay to measure cell envelope permeability in wildtype, ΔlmeA, and the complement strains. Time measured in minutes. *** indicates statistical significance

Δ*lmeA* had an increased uptake in rate and amount of ethidium bromide relative to WT and the complement. This data is in agreement with the antibiotic sensitivity data, indicating that Δ*lmeA* indeed has a defective cell envelope
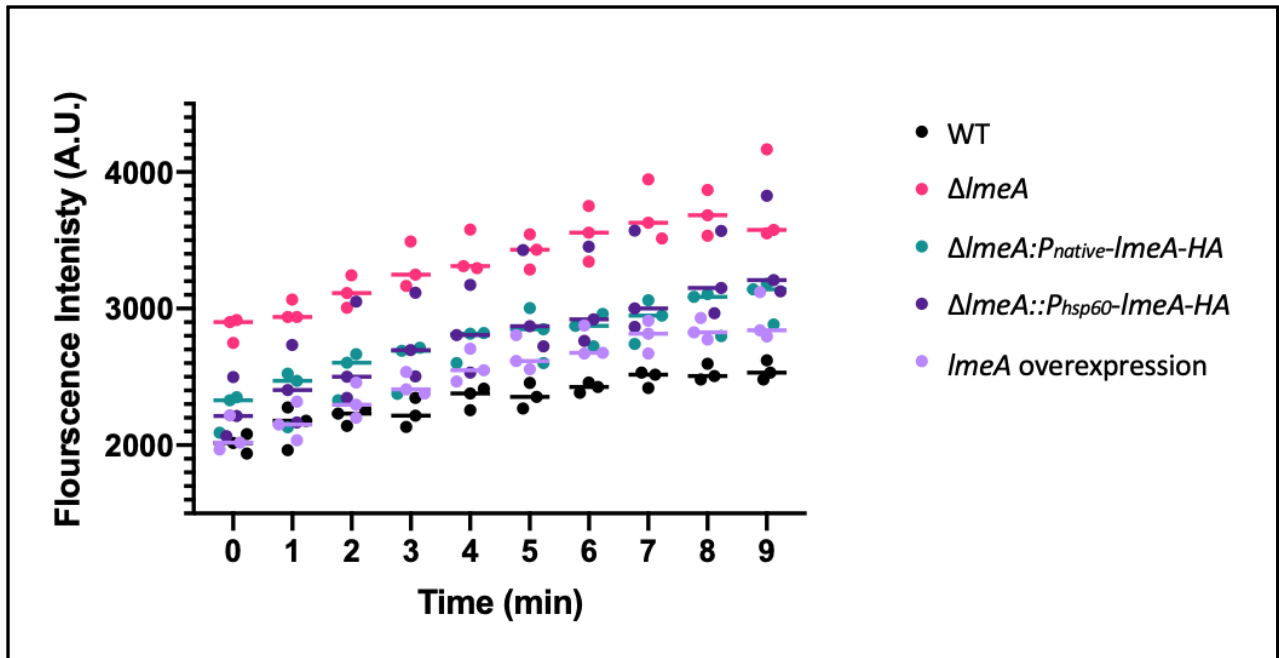
Figure 2.3: Ethidium Bromide Permeability Assay Wildtype, Δ*lmeA*, complements, and an overexpression strain were tested for permeability against 20 µM ethidium bromide. OE: overexpression.

As in Figure 2.2, WT was the least permeable while Δ*lmeA* showed the most permeability. Interestingly, the *lmeA* overexpression strain did not decrease ethidium bromide uptake relative to WT the way the overexpression strain improved antibiotic resistance.

2.4 Capsule Visualization

In Table 2.5, WT showed an increase in antibiotic resistance in the absence of tween, indicating that WT has an intact capsule that is disturbed by the presence of a detergent. Δ*lmeA*'s IC90 was unaffected by the presence of tween, leading us to speculate that the mutant already had a defective capsule.

To test this hypothesis, the capsule of WT and Δ*lmeA* was determined by the mannan and glucan binding FITC fluorescent-conjugated lectin, Concanavalin A and visualized using

19

fluorescence microscopy. No tween was used in the growing of these strains to minimize capsule disruption. Below are representative images of capsule staining.
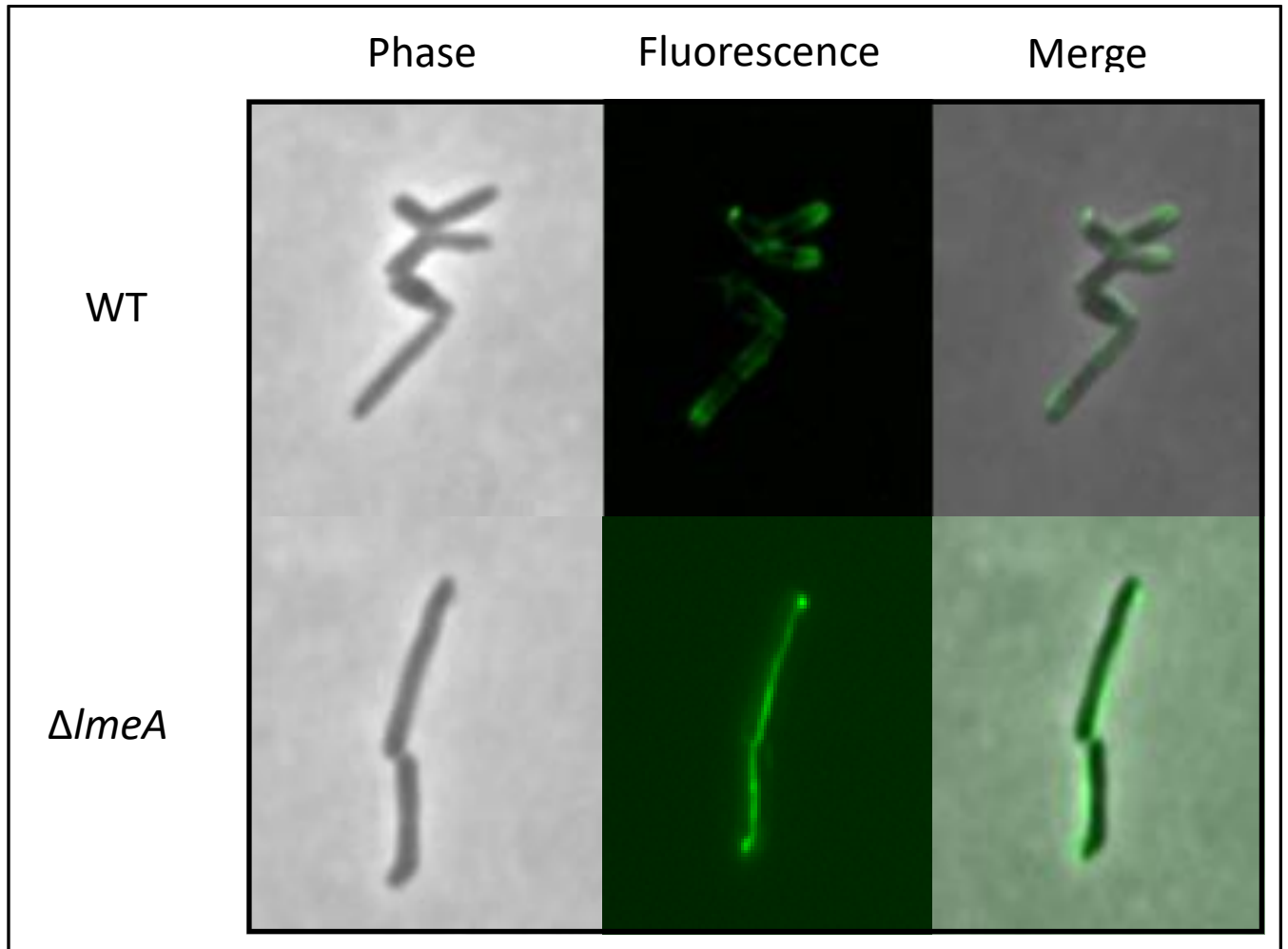
Figure 2.4: Capsule Visualization Capsules visualized using FITC-conjugated Concanavalin A binding lectin after one second exposure.

As this data was reproducible, it is clear that Δ*lmeA* has a defective capsule. WT shows a mostly polar with some sidewall staining. Δ*lmeA* shows capsule staining through the length of the cell, but only on one side of the cell. This indicates that LmeA may play a role in the distribution of mannans and glucans in the capsule layer.

LmeA has previously been shown to be important for MptA stabilization during stress conditions[27]. For this reason, we decided to investigate the capsule staining of a strain lacking *mptA* to see if it has a similar phenotype. To do this, we used an anhydrotetracycline (ATC)-inducible promoter to silence the *mptA* gene. It was also of interesting to investigate an *mptA* knockdown strain in an Δ*lmeA* background to see which would have the dominant phenotype.
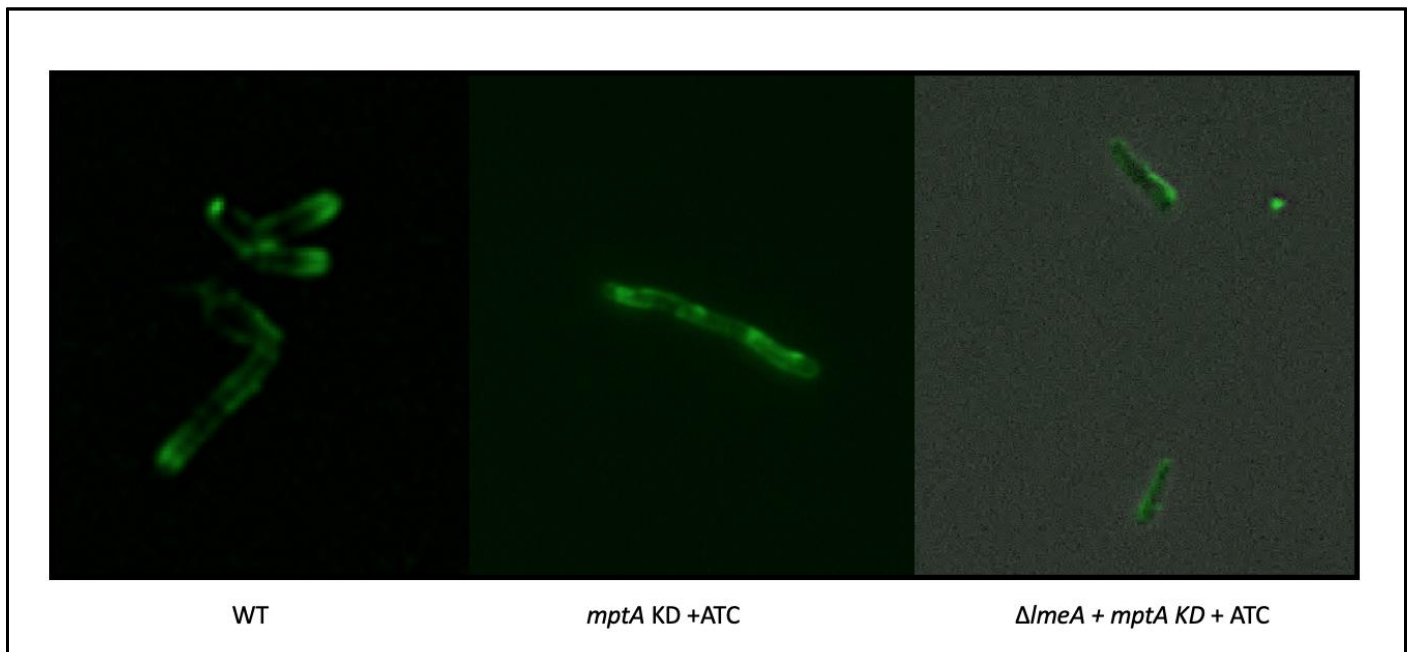
Figure 2.5: Capsule Visualization The capsules of an *mptA* knockdown strain and an *mptA* knockdown Δ*lmeA* strain were visualized using Concanavalin A and fluorescent microscopy.

The ATC-inducible *mptA* knockdown strain showed a unique phenotype relative to WT and Δ*lmeA* with no clear pattern for capsule staining. There seems to be patches with some foci all throughout the cell as opposed to the poles as seen in WT, or one-sided staining as in Δ*lmeA*. When ATC was added to the *mptA* knockdown Δ*lmeA* strain, the Δ*lmeA* phenotype was

21

dominant, showing only sidewall staining along one side of the cell. According to this one-sided sidewall staining, LmeA plays a unique role in capsule formation relative to MptA.

2.5 Protein Expression During Starvation

Previously, it has been shown that LmeA plays an important role during stress conditions, including starvation[27]. For this reason, it was of interest to investigate general protein expression relative to WT in log and starvation conditions. This process was started by making sucrose gradients of WT and Δ*lmeA* during log phase and starvation in order to compare protein content in the cytoplasm, the IMD, and the PMCW. In a sucrose gradient fractionation, fractions one and two are cytoplasmic. Fractions four through six are IMD and the remaining fractions seven through twelve are PMCW. Next, a bicinchoninic acid (BCA) assay was done in triplicate to standardize protein content before loading onto an SDS-PAGE gel. After equal amounts of protein were loaded onto each lane of the gel, the protein profile was visualized by silver staining.

	WT F3	WT F4	WT F5	WT F6	WT F7	WT F8	Δ*lmeA* F3	Δ*lmeA* F4	Δ*lmeA* F5	Δ*lmeA* F6	Δ*lmeA* F7	Δ*lmeA* F8
Averaged Value of Triplicate	0.12	0.096333	0.094	0.084333	0.082	0.083667	0.114667	0.103667	0.094333	0.085333	0.083	0.083333
µl of Sample	8.2	10.21	10.47	11.67	12	11.76	8.58	9.49	10.43	11.53	11.86	11.81
µl of Water	3.8	1.79	1.53	0.33	0	0.24	3.42	2.51	1.57	0.47	0.14	0.19

Table 2.6: BCA Assay for Log-Phase Sucrose Gradient Fractions Values are wavelength 562 nanometers.

	WT F3	WT F4	WT F5	WT F6	WT F7	WT F8	Δ*lmeA* F3	Δ*lmeA* F4	Δ*lmeA* F5	Δ*lmeA* F6	Δ*lmeA* F7	Δ*lmeA* F8
Averaged Value of Triplicate	0.099667	0.089333	0.089333	0.085	0.082667	0.083	0.109	0.095	0.097333	0.089667	0.086	0.085
µl of Sample	9.87	11.01	11.01	11.58	11.9	11.86	9.03	10.36	10.11	10.97	11.44	11.58
µl of Water	2.13	0.99	0.99	0.42	0.1	0.14	2.97	1.64	1.89	1.03	0.56	0.42

Table 2.7: BCA Assay for Starvation Sucrose Gradient Fractions Values are wavelength 562 nanometers.
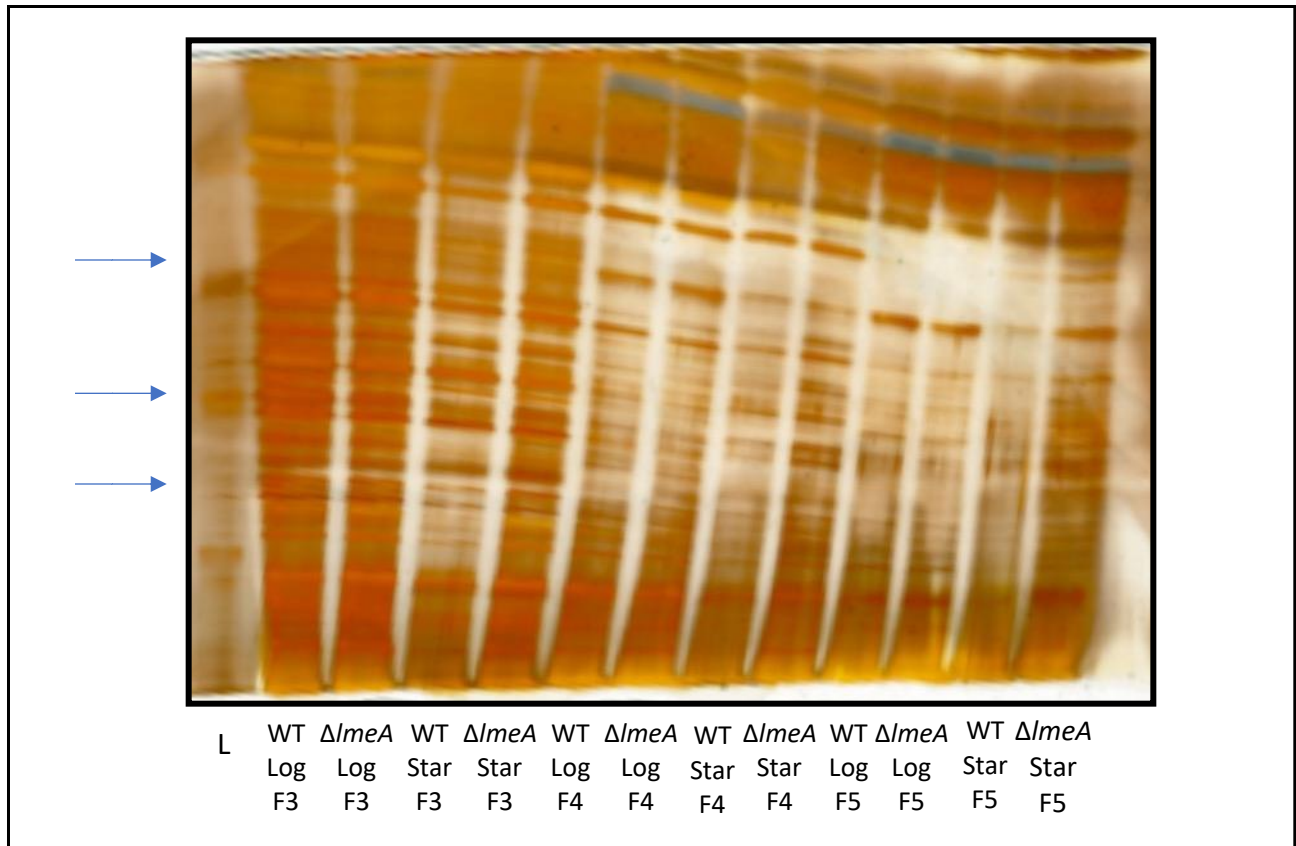
Figure 2.6: Silver Staining of WT and Δ*lmeA* Fractions 3-5 Log and Starvation Blue arrows indicate changes in specific protein bands.

The above silver staining shows differential protein expression not only between WT and Δ*lmeA*, but also between log and starvation phase. For fractions three through fractions five, Δ*lmeA* starvation seems to show increased protein content relative to WT log phase fractions, WT starvation fractions, and Δ*lmeA* log phase fractions. Although LmeA is a PMCW protein (fractions eight through twelve in a sucrose gradient), there are still changes in specific protein content that are pointed out by the blue arrows in the figure above.
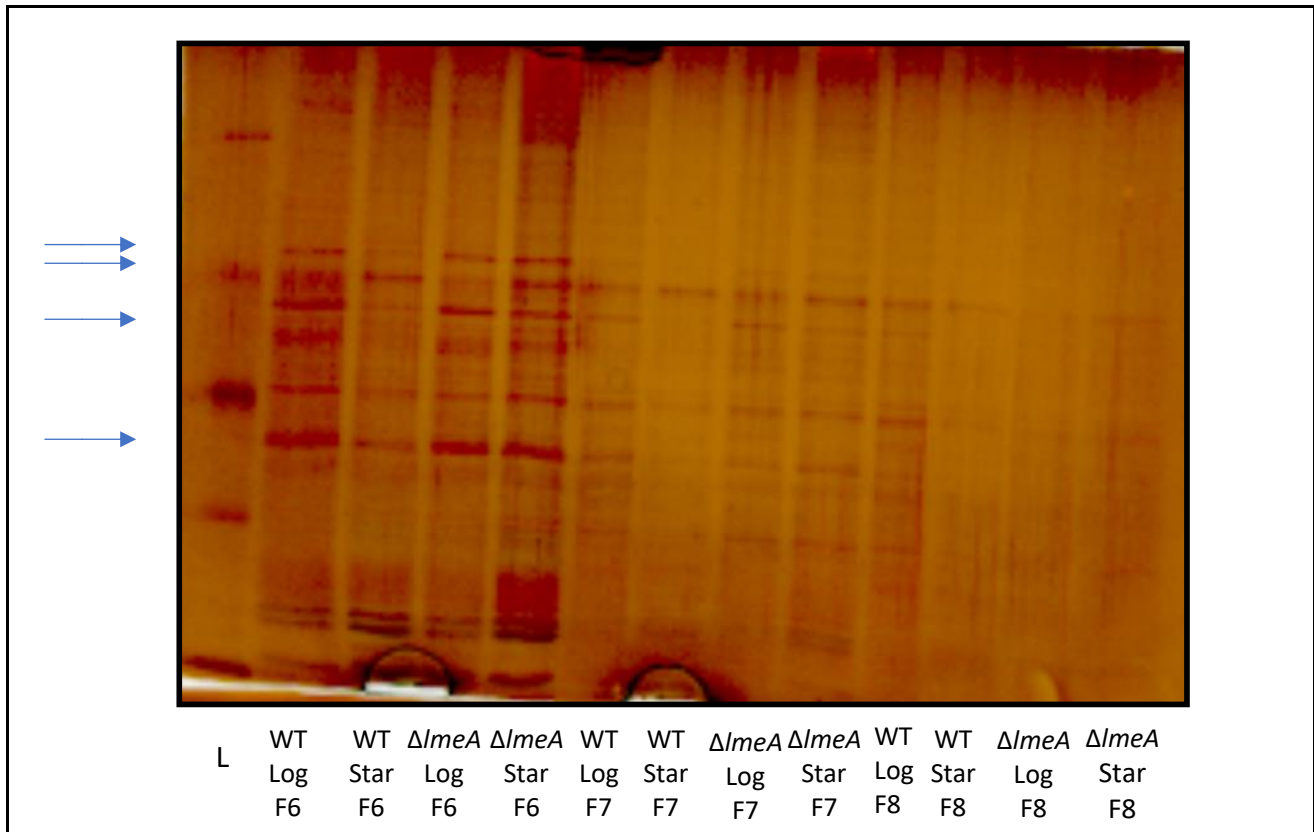
Figure 2.7: Silver Staining of WT and Δ*lmeA* Fractions 6-8 Log and Starvation Blue arrows indicate changes in specific protein bands.

In fractions six through eight, there are also changes in protein content between WT and Δ*lmeA*. In fractions six, some of the upper bands and the lower thick band are upregulated in Δ*lmeA*. The fractions further from the cytoplasm tend to have less protein, which is shown here by the low protein content in fractions seven and fractions eight. Changes in specific protein bands are indicated by the blue arrows in the figure above.
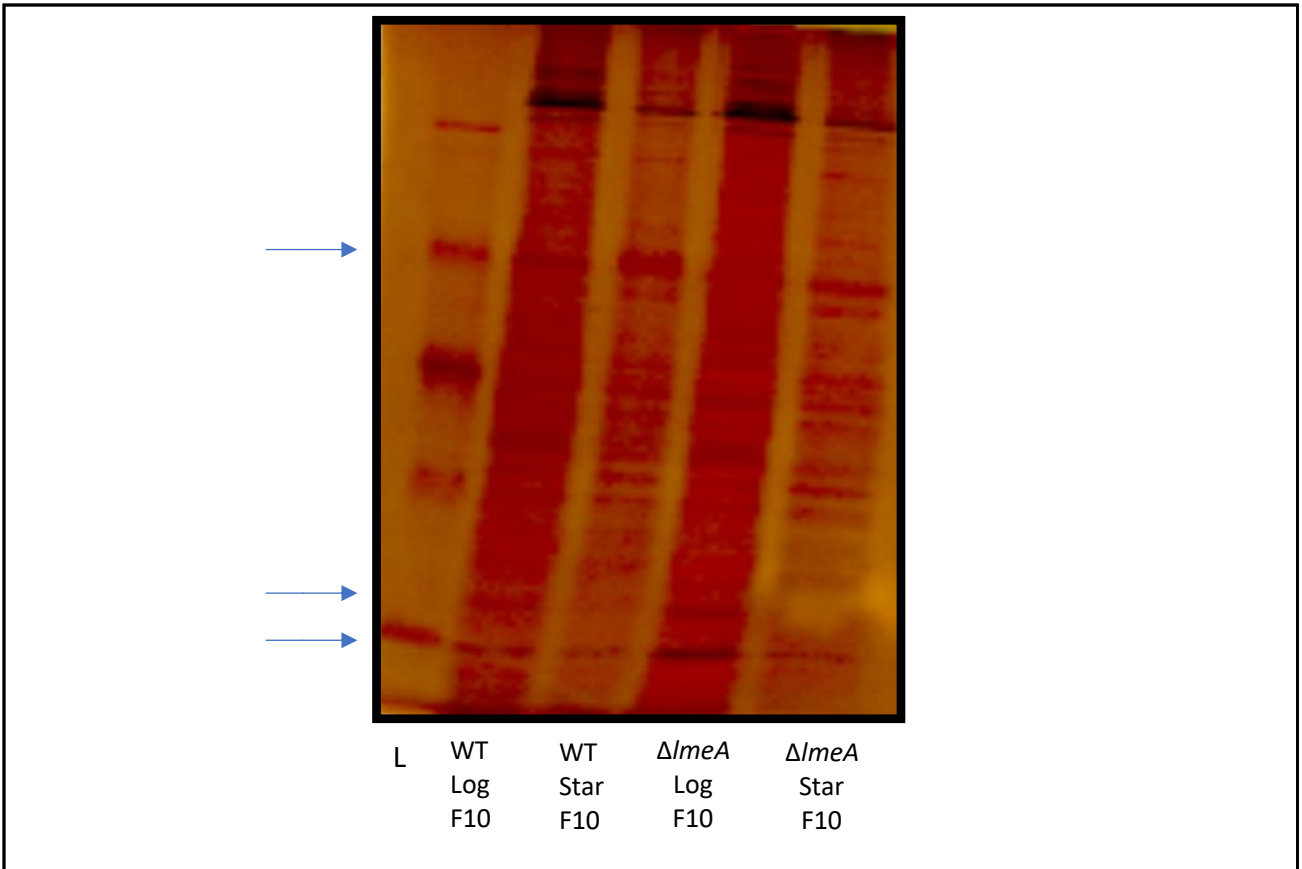
Figure 2.8: Silver Staining of WT and Δ*lmeA* Fraction 10 Log and Starvation Blue arrows indicate changes in specific protein bands.

As stated before, LmeA is a PMCW protein, so it was of interest to look at protein content changes in a PMCW fraction. Fraction 10 from each sucrose gradient underwent protein precipitation in order to visualize during silver staining. In these fractions, contrary to the pattern seen in Figure 2.6. In Figure 2.8, Δ*lmeA* starvation fractions do not have more protein content relative to the other samples. In fact, in this fraction, WT log has the most protein content. Specific changes in bands are indicated by the blue arrows. Taken together, these figures indicate that Δ*lmeA* changes the protein profile in different ways, depending on the cellular fraction location.

Chapter 3
LmeA Localization and Cell-Envelope Binding Properties

3.1 Previous Data Within This Aim

Understanding the binding behavior and localization of a protein can give important clues to its function. For this reason, it is of interest to investigate the binding of LmeA. Previously, it has been shown that LmeA binds phospholipids His-LmeA was purified from an IPTG inducible *E. coli* expression vector. In an ELISA setting, LmeA was able to bind to phosphatidylinositol, phosphatiphatidylethanolamine, and phosphatidic acid. Interestingly, LmeA was only able to bind to these lipids in the presence of *E. coli* lysate. LmeA-HA was also shown to localize to PMCW fractions *in-vivo* in a sucrose gradient setting[35].

3.2 LmeA Binding *in-vitro*

LmeA is predicted to have a signal peptide and is secreted into periplasmic face of the plasma membrane (Figure 3.1). Whether or not the signal peptide gets cleaved or LmeA remains anchored to the plasma membrane is still unknown. To further investigate LmeA localization and binding, it is of interest to determine LmeA's localization *in-vitro*, when it has a "choice" to bind to any cell envelope component as opposed to being trapped in its natural location, the periplasm. To investigate this, His-LmeA was purified from an IPTG inducible *E. coli* expression vector (Figure 3.2). The protein was purified via a nickel affinity column and eluted using an elution buffer containing HEPES and imidazole.
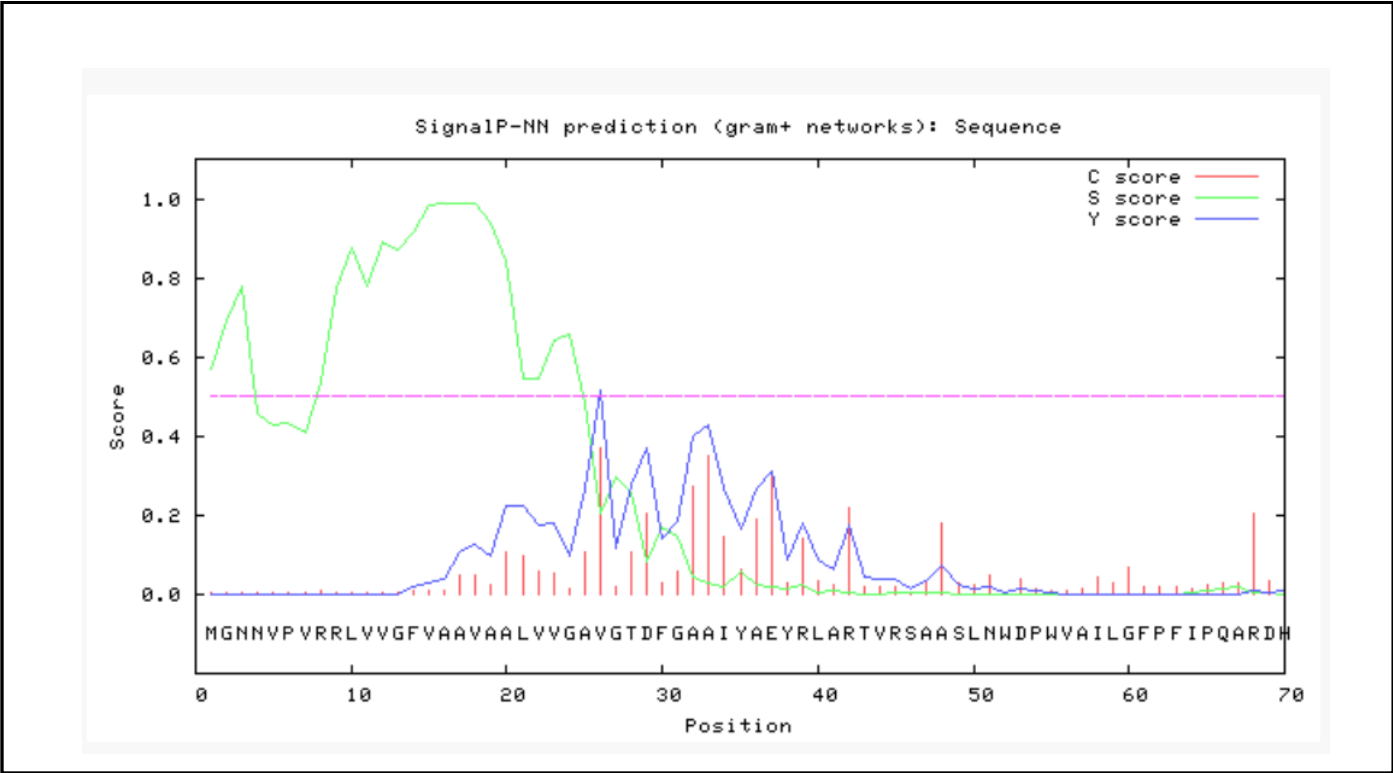
Figure 3.1: LmeA has a Predicted Signal Peptide Figure generated using SignalP 3.0. Neural network model. Signal peptide is likely cleaved between amino acid 27 and 28.
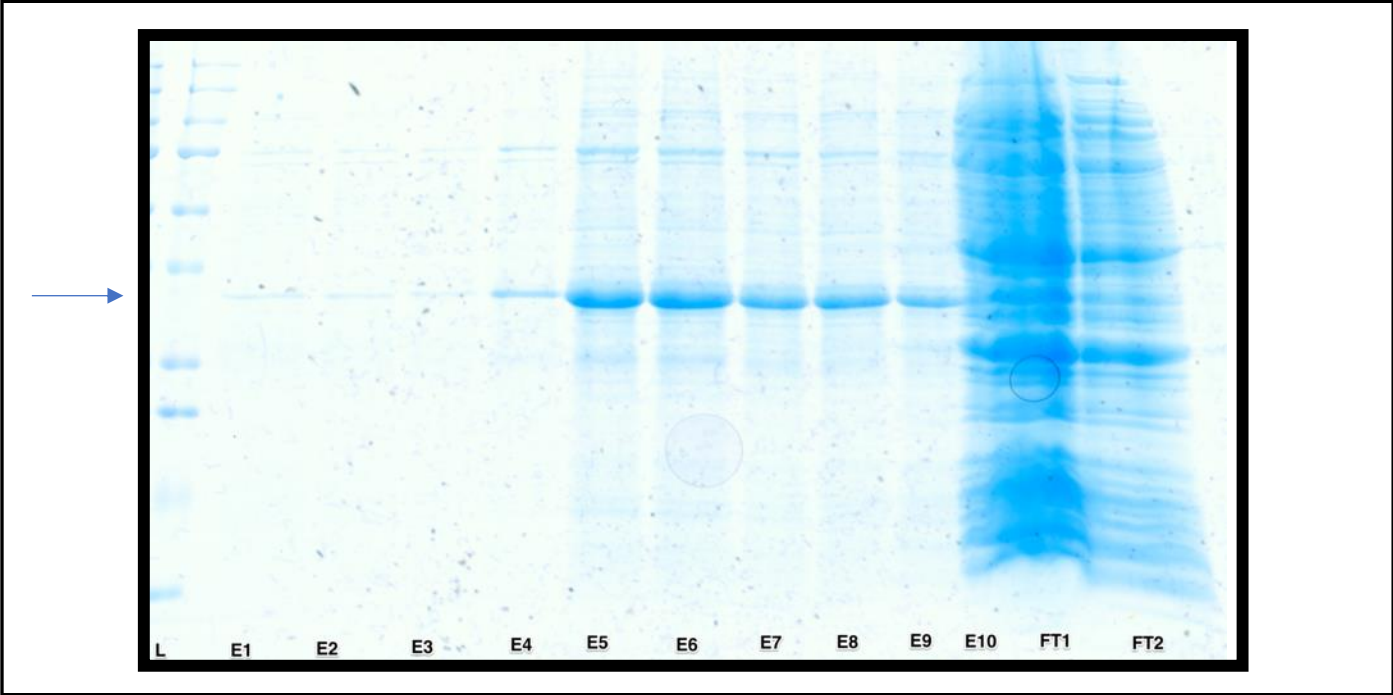
Figure 3.2: Purification of LmeA from _E. coli_ Expression Vector. L: Ladder, E: Elution, FT: Flowthrough. LmeA is a 29 kDa protein indicated by the blue arrow.

Next, this purified His-LmeA was added to WT cell lysate and incubated for half an hour

at 37°C. LmeA was also added to buffer and ran identical to the sample as a control. These

mixtures were then added to a sucrose gradient and fractionated after centrifugation. Each

fraction was then run on an SDS-PAGE gel and a Western blot was done to probe for the protein

of interest (Figure 3.4). The same lysate was used to probe for other cell envelope proteins to

serve as markers for the cytosol, the IMD, and the cell envelope.
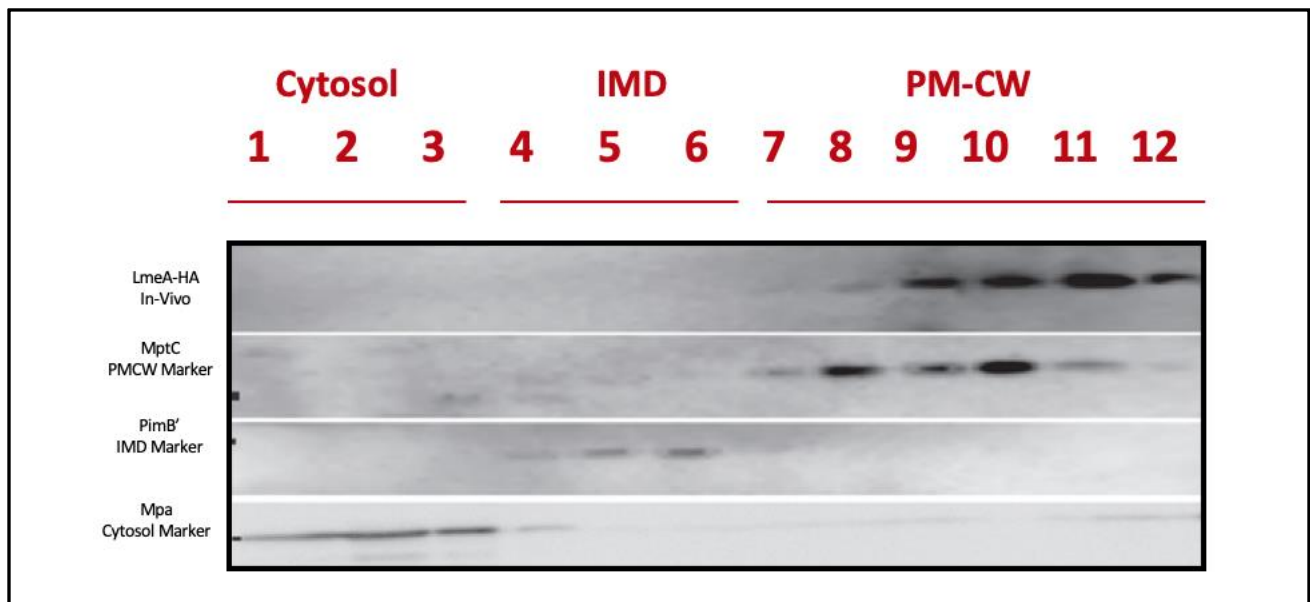
Figure 3.3: Western Blot Localization of LmeA-HA *In-vivo* After Sucrose Gradient Ultra-Centrifugation. Figure by Kathryn Rahwles[35].
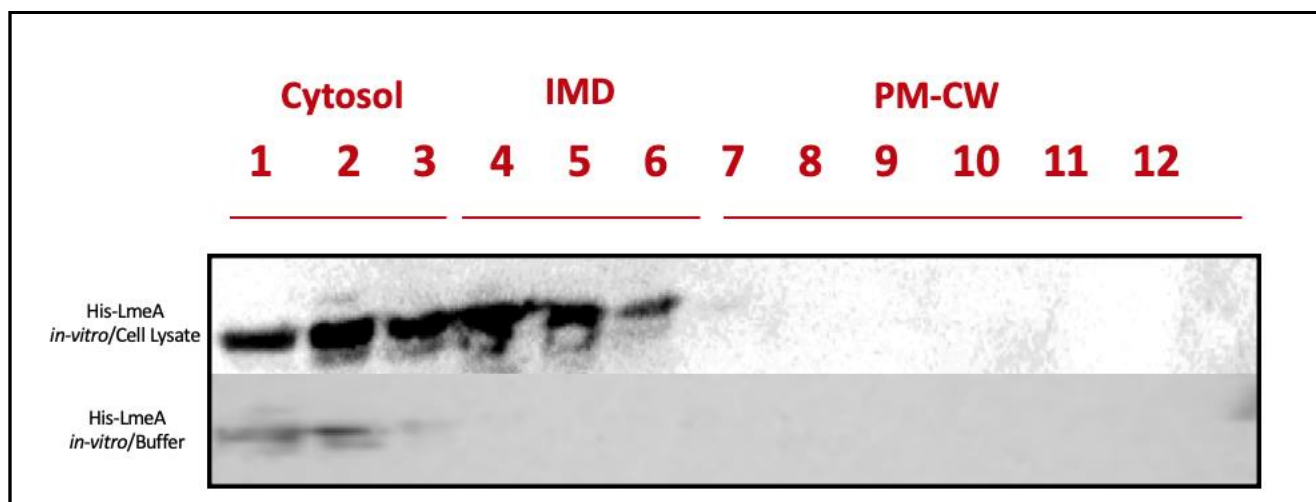
Figure 3.4: Western Blot Localization of LmeA-HA *in-vitro* After Sucrose Gradient Ultra-Centrifugation

LmeA showed differential localization *in-vitro* vs *in-vivo*. *In-vivo*, LmeA localized to fractions seven through twelve- PMCW fractions and co-localized with the PMCW marker, MptC. When LmeA was added to buffer and no cell lysate was present, it remained in cytosolic fractions and co-localized with a cytosol marker, Mpa. When LmeA was mixed with lysate, it bound to only IMD fragments and co-localized with the IMD marker, PimB'. This indicates that only plasma membrane, and not any cell wall component, is required for binding.

3.3 LmeA Binds to Spheroplasts

To further investigate LmeA binding activity, spheroplasts were made from WT *M. smegmatis* cells. Glycine was used to inhibit the production of peptidoglycan and lysozyme was added to remove any existing peptidoglycan. Microscopy was done before and after these additions to confirm the presence of spheroplasts (Figure 3.5).
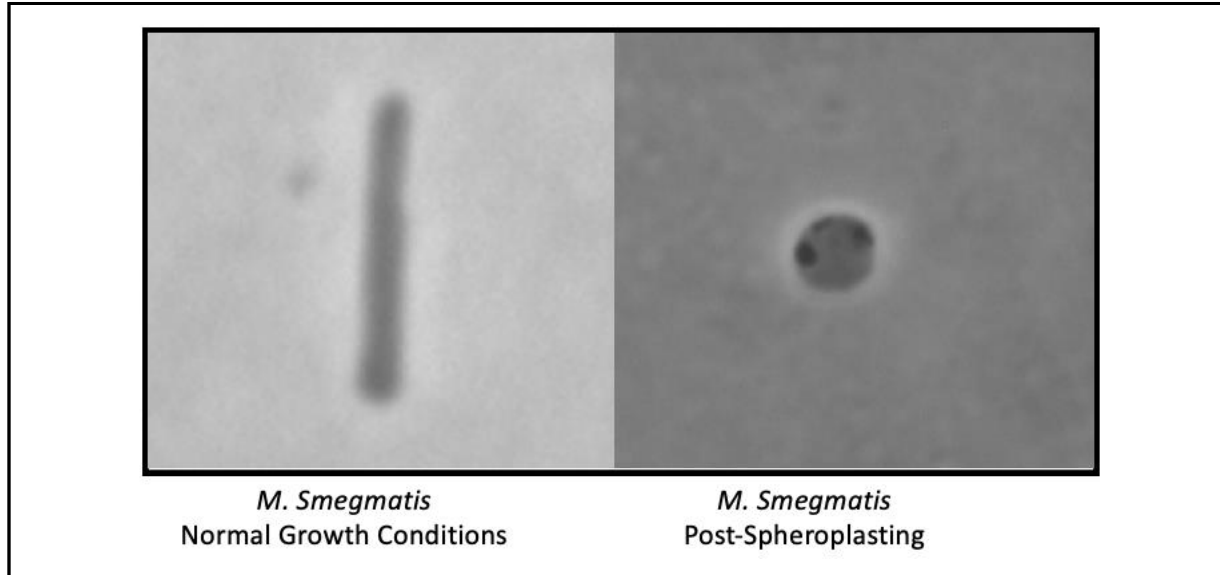
Figure 3.5: *M. smegmatis* **cells before (left) and after (right) spheroplasting**

Purified His-LmeA was then added to these spheroplasts and incubated for half an hour at 37°C. This mixture was then placed atop a sucrose gradient, centrifuged, and fractionated. Each fraction was run on an SDS-PAGE gel, transferred to a membrane, and a Western blot was done to probe for the protein of interest as well as MptC, the PMCW marker, and PimB', the IMD marker (Figure 3.6).
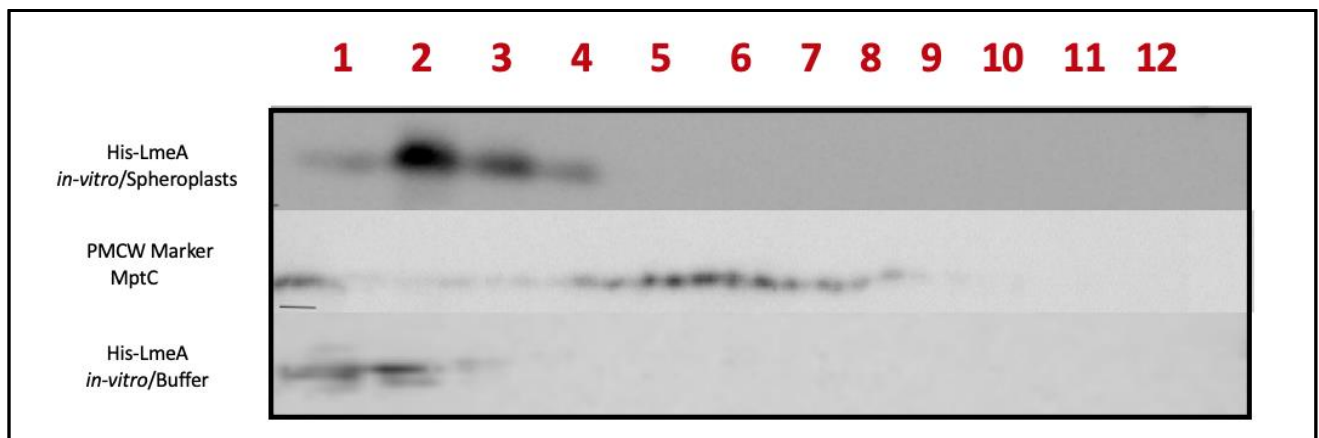
Figure 3.6: His-LmeA and MptC Localization after Spheroplast Formation

In vitro in rod-shaped cells, LmeA localizes to fractions containing plasma membrane free of cell wall components and migrates differentially from the PMCW marker MptC. This indicated that only plasma membrane is necessary for LmeA binding, and that LmeA shows differential binding from typical PMCW proteins. This spheroplast binding assay (Figure 3.6) is a secondary confirmation of these previous findings. Indeed, LmeA was able to bind spheroplasts and also showed differential localization from the PMCW marker. Interestingly, PimB', an IMD marker, was unable to be detected upon spheroplast formation.

As another confirmation that LmeA binds spheroplasts, an ELISA was done. Spheroplasts were made and added to the bottom of the 96-well ELISA plate. To measure background binding, a negative control of isopropanol was added in place of spheroplasts. Purified LmeA was either mixed with untransformed *E. coli* lysate or not, and these mixtures were added. After incubation, the plate was read in a spectrophotometer at 650 nanometers. LmeA was able to bind to spheroplasts, with or without *E. coli* lysate although binding was more robust in the presence of the lysate. There was also some binding in the negative control. LmeA was able to bind to spheroplasts, with or without *E. coli* lysate although binding was more robust in the presence of the lysate. There was also some binding in the negative control. LmeA was able to bind to spheroplasts, with or without *E. coli* lysate although binding was more robust in the presence of the lysate. There was also some binding in the negative control

As another confirmation that LmeA binds spheroplasts, an ELISA was done (Figure 3.7). Spheroplasts were made and added to the bottom of the 96-well ELISA plate. To measure background binding, a negative control of isopropanol was added in place of spheroplasts. Purified LmeA was either mixed with untransformed *E. coli* lysate or not, and these mixtures were added. After incubation, the plate was read in a spectrophotometer at 650 nanometers.

LmeA was able to bind to spheroplasts, with or without *E. coli* lysate although binding was more

robust in the presence of the lysate. There was also some binding in the negative control.
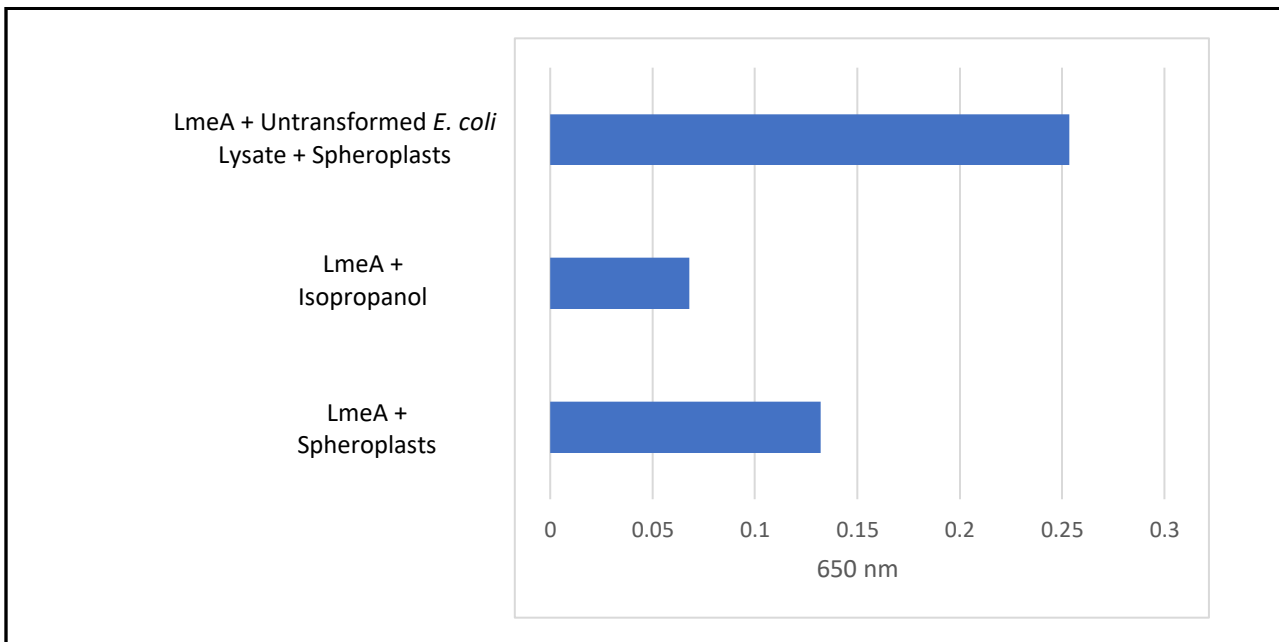
Figure 3.7: LmeA Binds to Spheroplasts in an ELISA Setting Values read at 650 nanometers.

Chapter 4
LmeA's Role in MptA Stabilization and Possible Interactions with ThiX

4.1 Previous Data Within This Aim

It has previously been shown that during stress conditions, LmeA plays a role in MptA stabilization[27] . During starvation and stationary phase, MptA degrades over time in ΔlmeA while MptA levels stay constant in WT. It has also been found that the transcription of *lmeA* is upregulated during stress conditions.

4.2 Δ*lmeA* Has a Growth Delay After Starvation

As mentioned before, Δ*lmeA* does not have a growth delay under normal laboratory conditions. Since LmeA has previously been shown to play an important role during stress, it was of interest to determine if Δ*lmeA* struggles to recover after stress conditions. To do so, we grew WT and Δ*lmeA* to log phase, pelleted, washed, and resuspended in phosphate-buffered saline (PBS), starved for 24 hours, and placed back into 7H9 Middlebrook media to allow a chance for recovery. Optical density (OD) was measured every few hours to monitor growth (Figure 4.1).
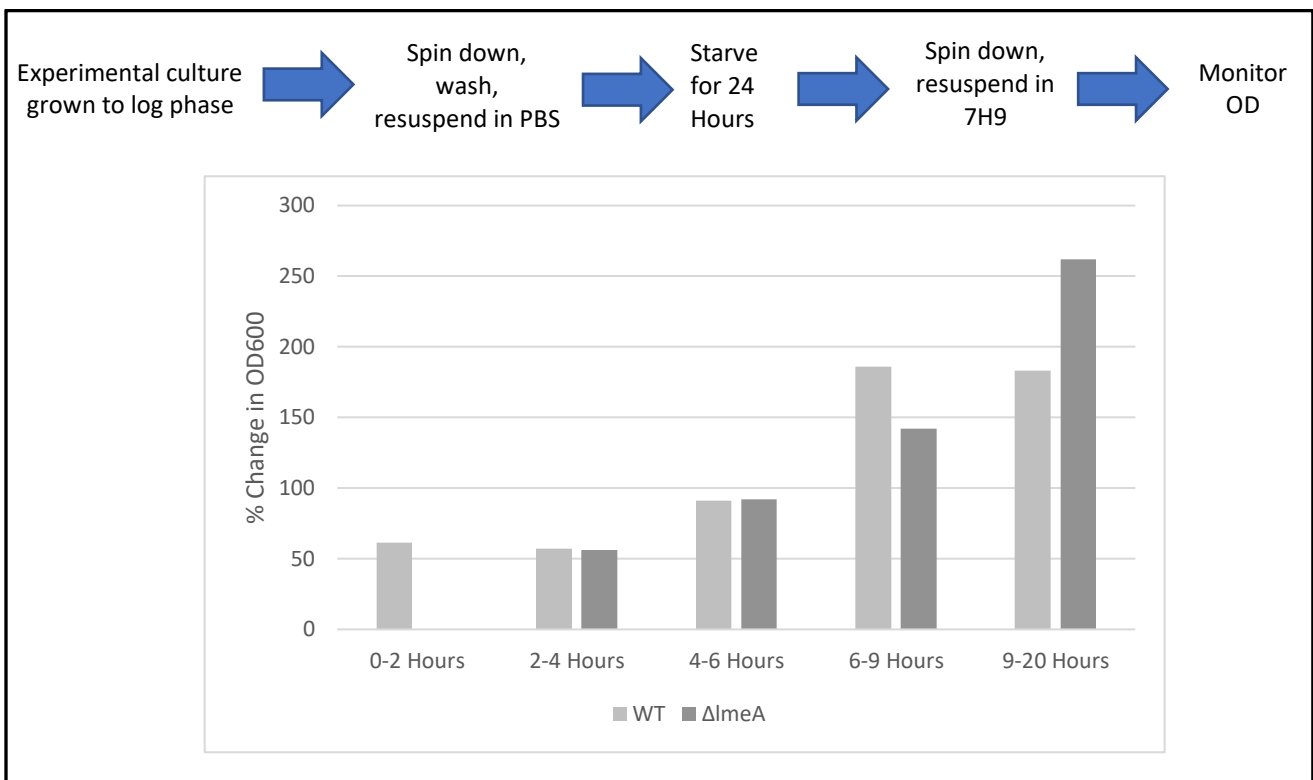
Figure 4.1: Δ*lmeA* Has a Growth Lag After Starvation Percent change calculated with the following equation: % change = [OD2-OD1]/OD1

Δ*lmeA* did not grow at all for the first two hours after starvation. From two hours to six hours, WT and Δ*lmeA* grew at the same rate. From six to nine hours, Δ*lmeA* lagged in growth behind WT. Finally, between nine and twenty hours, Δ*lmeA* not only caught up in growth rate, but actually surpassed WT in growth. This data shows that Δ*lmeA* has a lag in growth that only occurs after stress.

OD is not the most reliable method to measure cell viability as cell debris and other factors can increase optical density, artificially inflating the growth rate. As a secondary confirmation, this recovery growth curve was done in a different format. Instead of using OD to monitor growth, resazurin was used to measure cell viability (Figure 4.2).
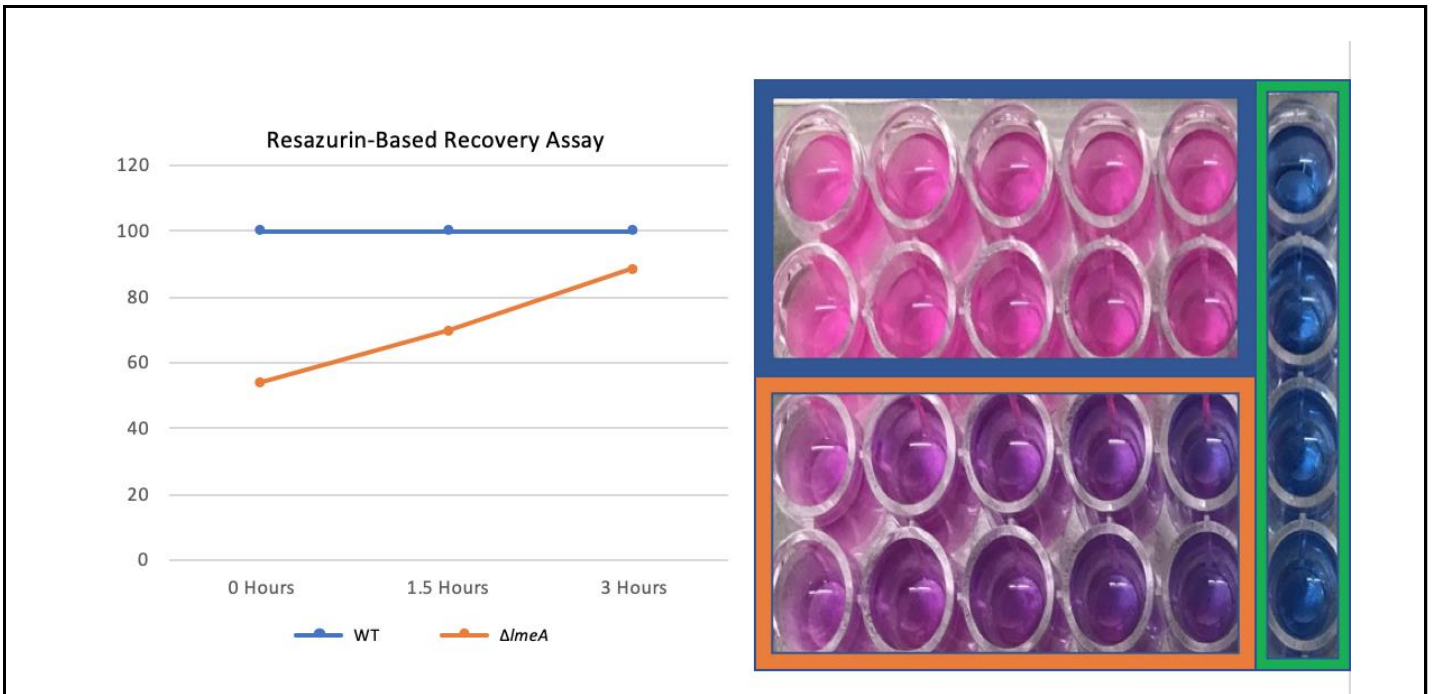
Figure 4.2: Δ*lmeA* Has a Growth Lag after Starvation In the photo on the right, the orange box indicates Δ*lmeA* replicates. The blue box indicates WT replicates. The green box indicates a negative control containing only media and resazurin. Photo taken at the 1.5 hour mark. On the left, y-axis shows percent growth normalized to WT.

These results show that Δ*lmeA* indeed does have a growth lag after a twenty-four-hour starvation period. When using the OD values from the spectrophotometer to read the 96-well plate, these values are converted to percent viability using an equation that requires a no-drug control. Since this is not a dose response assay, there is no no-drug control and instead, WT's average OD value was used for this number since WT's growth rate represents the non-variable growth rate. In other words, Δ*lmeA* was normalized to WT. It takes three hours for Δ*lmeA* to return to a normal growth rate. This can be visually seen in right panel of Figure 4.2, where Δ*lmeA* is much bluer than WT, indicating less growth.

4.3 Investigating LmeA as a Possible Thioredoxin Reductase

lmeA shares an operon with one other gene- *MSMEG_5786*. According to bioinformatics, this gene encodes a putative thioredoxin. Thioredoxins are small redox proteins that are present in nearly all organisms. Thioredoxins operate by reducing disulfide bridges between cysteines in other proteins. They are typically characterized by their CXXC amino acid motif and have a characteristic thioredoxin fold in their tertiary structure. *MSMEG_5786* (*thiX)* is 465 base pairs long and encodes a protein that 16260.6 daltons. *thiX* is well conserved in mycobacteria, with the characteristic CXXC motif present throughout *M. tuberculosis*, *M. smeg*, *M. leprae*, *M. bovis*, and *M. marinum* (Figure 4.3). The ortholog in *M. tb* is Rv0816c.

Operons are two or more genes that share the same promoter and are transcribed simultaneously as one large mRNA. Genes are typically grouped in operons when they encode proteins that share a common purpose. Because of this coupled with the fact that LmeA has been shown to play a role in stress response, it is of interest for us to investigate LmeA's relation to ThiX.
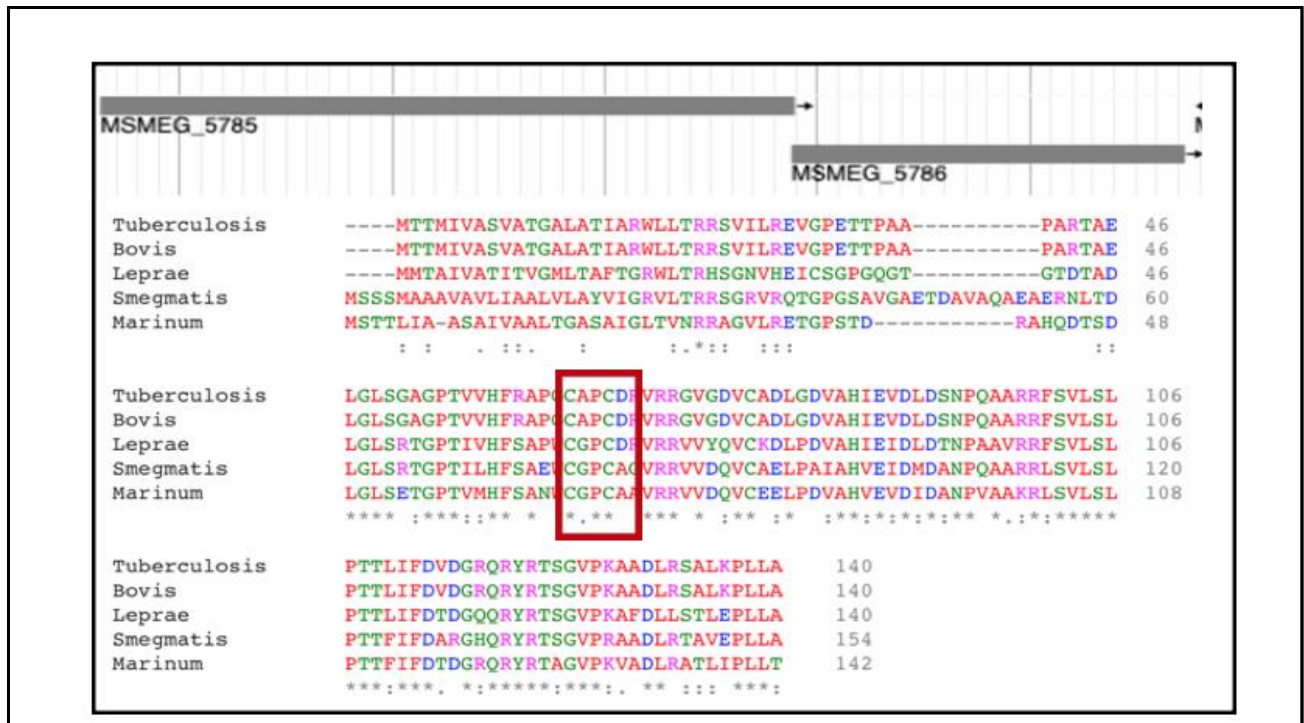
Figure 4.3: *thiX* **is a Conserved Gene Throughout Mycobacteria** Top panel shows ThiX's location in the operon. Bottom panel shows homology between species of mycobacteria. Top panel generated via Mycobrowser.com. Bottom panel generated by NCBI Protein Blast. Red box indicates conserved CXXC motif that is characteristic of thioredoxins.

One possible hypothesis is that LmeA acts as a thioredoxin reductase, reducing ThiX.

Going off this theory, it is possible that ThiX is responsible for degrading MptA in Δ*lmeA* during

stress conditions. Interestingly, MptA has well conserved cysteine residues that could possibly be

forming disulfide bridges for this thioredoxin to reduce (Figure 4.4).
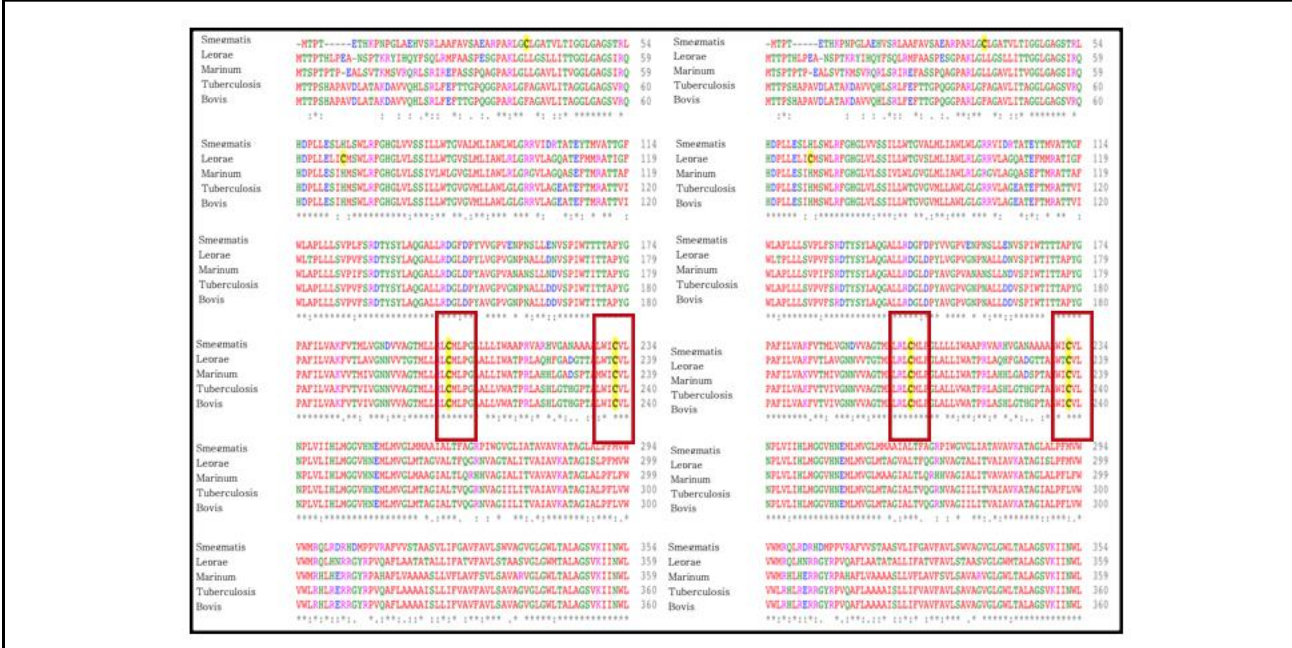
Figure 4.4: MptA has Conserved Cysteine Residues Throughout Mycobacteria Figure generated using NCBI Protein BLAST. Boxes indicate conserved cysteines residues that could form possible disulfide bridges.

To investigate this, we decided that two new strains should be made: *lmeA-HA-ΔthiX* and *ΔlmeA-ΔthiX*. These strains can be used for a variety of assays to check for changes in LmeA localization and MptA levels during stress conditions. The first step was to design primers for HiFi cloning and amplify upstream and downstream of the genes of interest using polymerase chain reactions (PCR).
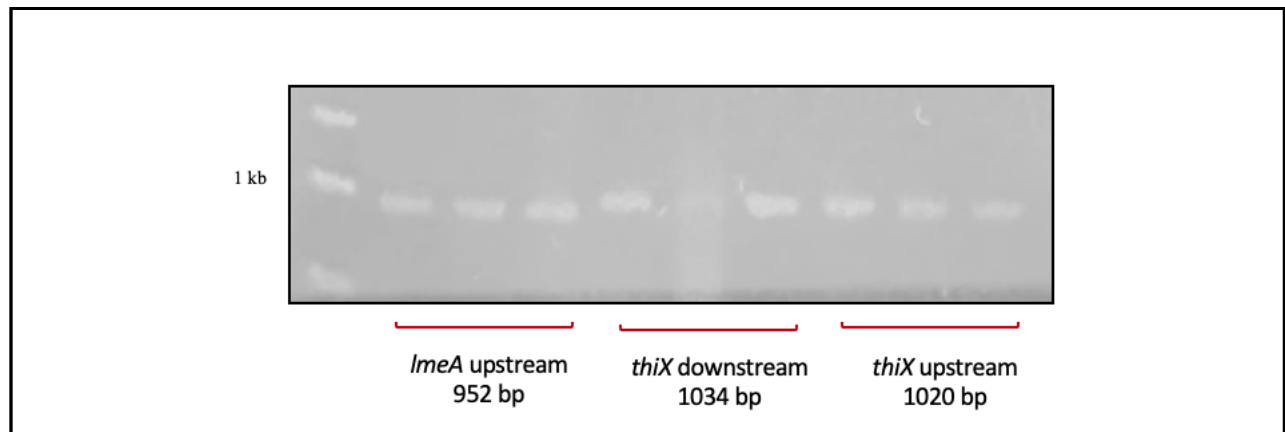
Figure 4.5: PCR Amplification of Upstream and Downstream Genes of Interest L: Ladder. Lanes 1, 2, 3: *lmeA* upstream, 952 bp expected size. Lanes 4, 5, 6: *thiX* downstream, 1034 bp expected size.

After successful PCR amplification, the fragments were purified via PCR cleanup and the proper fragments were inserted into a digested vector via HiFi cloning according to the construct wanted. This ligated plasmid was then heat shocked into competent *Escherichia coli* cells and grown on lysogeny broth (LB) plates containing hygromycin to select for the plasmid containing a hygromycin resistant cassette. Colonies were picked and grown in TBK liquid medium planktonically at 37°C overnight. These candidate plasmids were purified from the cells and digested with HindIII restriction enzyme to confirm the construct.
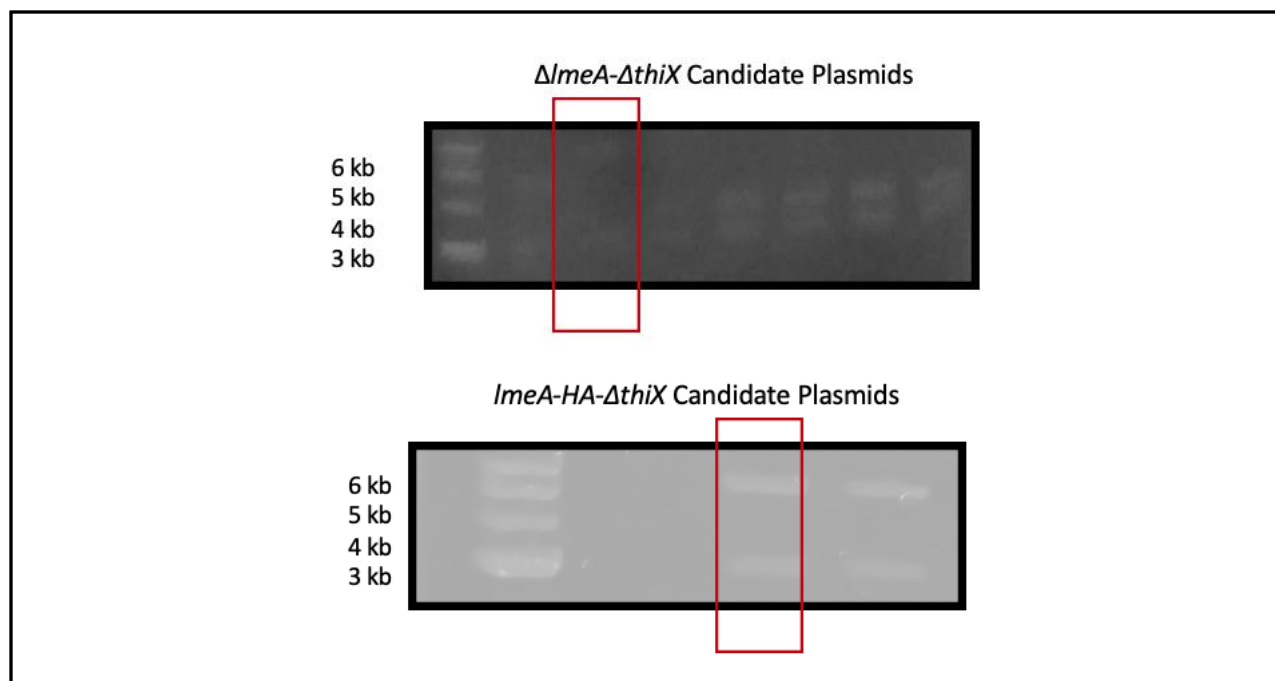
Figure 4.6: HindIII Restriction Enzyme Digest of Candidate Plasmids Top Panel: Δ*lmeA*-Δ*thiX* candidates, expected size: 3163 bp & 6747 bp. Plasmid #2 chosen and sent for sequencing. Bottom Panel: *lmeA-HA-ΔthiX* candidates. Expected size: 3163 bp, 5729 bp. Plasmid #1 chosen and sent for sequencing.

Candidate plasmids showing the proper band sizes after restriction enzyme digest were sent for Sanger sequencing for secondary confirmation and both plasmids came back as the confirmed construct. As of this thesis being written, only Δ*lmeA*-Δ*thiX* has been successfully electroporated into electrocompetent *M. smegmatis* cells. The colonies from electroporation were confirmed for the double crossover event via sucrose sensitivity and hygromycin resistance and frozen stock was made. Genomic DNA was extracted, and primers were designed outside the inserted region to confirm the strain. The PCR came out successfully and two identical strains were confirmed to be our constructs. No testing has yet been done on this strain.
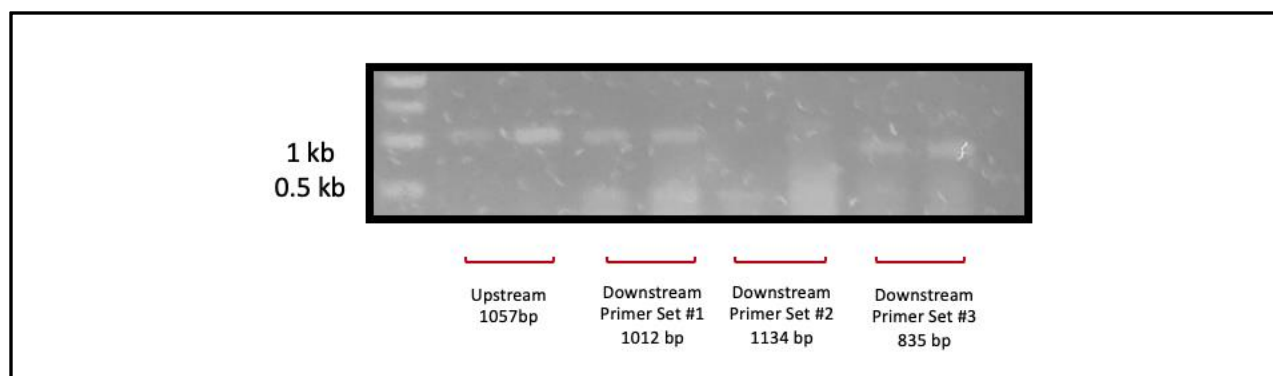
Figure 4.7: PCR Amplification of Extracted Genomic DNA to Confirm Double Knockout Strain L: Ladder. Lanes 1 & 2: Upstream fragment, expected size 1057 bp. Lanes 3 & 4: Primer set #1 to amplify downstream fragment, expected size 1012 bp. Lanes 5 & 6: Primer set #2 to amplify downstream fragment, expected size 1134 bp. Lanes 7 & 8: Primer set #3 to amplify downstream fragment, expected size 835 bp.

An AMB Master's student, Audrey Della Valle, has cloned *thiX* into an *E. coli* expression vector and successfully purified ThiX. I am in possession of purified LmeA. LmeA will be tested for thioredoxin reductase activity by testing to see if the protein is able to reduce 5,5'-dithiobis-(2-nitrobenzoic acid) using NADPH as a source of electrons. ThiX will be tested for thioredoxin activity against insulin.

Chapter 5
Discussion and Future Directions

This study aimed to further characterize LmeA by investigating antibiotic sensitivity, cell envelope permeability, protein expression during different conditions, capsule staining, binding, and its interactions with other proteins. Although this study made advances in the characterization of this protein, LmeA's exact function remains unclear.

It is interesting to note that although the suppressor mutants ($\Delta pimE$ with a point mutation in *lmeA* rendering it non-functional) restore colony size, the suppressor mutants do not recover in any other aspect. They are still sensitive to antibiotics, still more permeable to ethidium bromide relative to wildtype, and still have shorter lipomannan and lipoarabinomannan[35]. Perhaps it would be of interest to further study the relationship between this restored colony size with these altered phenotypes- why only colony size is restored when seemingly all other tested phenotypes do not recover. It is also interesting to note that these suppressor mutants do not become more sensitive to antibiotics relative to $\Delta pimE$ or $\Delta lmeA$. One would assume that not having both of these functional proteins would compound and exacerbate the already defective cell envelope and increase antibiotic sensitivity. Perhaps this could be another route of investigation.

$\Delta lmeA$ became more sensitive to antibiotics. This was expected because this mutant is unable to produce mature LM and LAM- important components for cell envelope integrity. Less expected was the increased antibiotic resistance seen in the three overexpression strains. Previously, it has been shown that in these overexpression strains, LM and LAM are more abundant. This leads us to conclude that the wildtype cell envelope has room for improvement- apparently increasing the abundance of LM and LAM translates into a more fortified cell

envelope. One study showed that *lmeA* is upregulated upon *M. tb* infections in mice, and this is in accordance with the pattern we are seeing. It is also worth noting these strains have different responses to antibiotics, depending on the antibiotic's target. In the *lmeA* overexpression strains, antibiotic sensitivity increased at a rate higher in macrolides than antibiotics with cell envelope targets. It is also worth noting that in the suppressor mutant strain complemented with overexpressed *lmeA*, antibiotic resistance is at an all-time high for erythromycin relative to the other strains tested. Another point to note is the difference in antibiotic sensitivity between clarithromycin and erythromycin. They are both macrolides- in fact, clarithromycin is just the new generation of erythromycin. Clarithromycin has been shown to be several-fold more active *in-vitro* than erythromycin. This supports the trend seen in the antibiotic resistance table. Clarithromycin resistance only increases six-fold at its peak while erythromycin increases ten-fold at its peak. Another point to be made with this antibiotic sensitivity data is its relation a previously done transposon mutagenesis. Wildtype and Δ*lmeA* underwent a transposon mutagenesis assay. As one can see below in Figure 5.1, Δ*lmeA* had fewer insertions in *MSMEG_2584*, a gene encoding a putative penicillin binding protein. This data is in accordance with the antibiotic sensitivity data showing Δ*lmeA* is sensitive to beta-lactams.
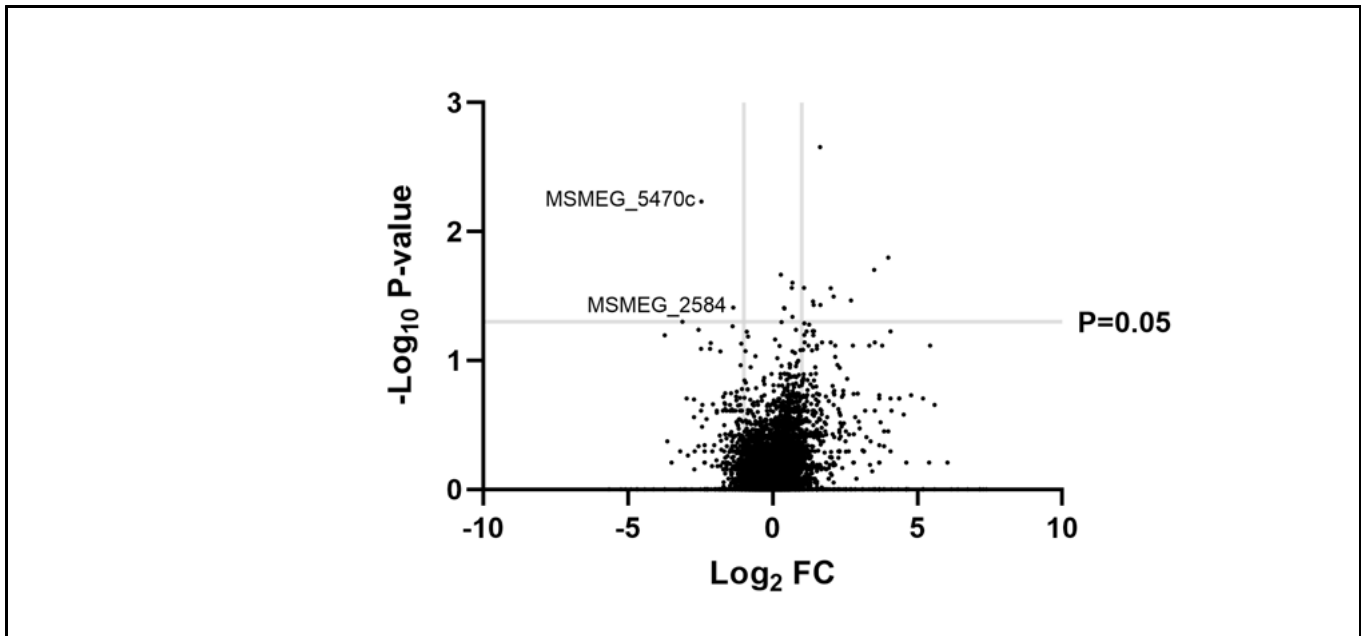
Figure 5.1: Transposon Mutagenesis Data Experiment done by Kathryn Rahlwes and analyzed by Hiro Kado.

It is also interesting to discuss temperature's effect on Δ*lmeA*. At higher temperatures, the fatty acid tails of phospholipids in the plasma membrane become less rigid, and this can lead to increased membrane fluidity. From 30°C to 37°C, Δ*lmeA* showed increased antibiotic sensitivity by more than 2.5-fold in the case of vancomycin while WT only increased by 0.5-fold. Perhaps the lack of LM and LAM exacerbates this membrane fluidity that follows an increase in temperature. It is unclear why the native complement struggles to restore antibiotic resistance. Perhaps it is the L5 integration site of the complemented *lmeA* gene that is responsible for this. This issue is exacerbated at 30°C- something that is not seen at 37°C. A western blot comparing LmeA-HA levels at these two temperatures would easily solve this question.

The presence or absence of the detergent tween did not have an effect on Δ*lmeA* antibiotic sensitivity, while WT was greatly affected. Since tween only physically interacts with the capsule, it leads us to believe that our mutant already has a defective capsule. If Δ*lmeA* naturally has a

defective capsule, the disturbance from tween will not have a significant effect on antibiotic sensitivity. The capsule staining that was done supports this hypothesis. Wildtype capsule staining showed mostly polar with some sidewall staining. Δ*lmeA* had a unique phenotype that showed the length of the sidewall being stained, but only on one side. This phenotype has been reproduced in three separate experiments. In addition, this Δ*lmeA* capsule phenotype is the dominant phenotype in an *mptA* knockdown-Δ*lmeA* strain. This leads us to believe that perhaps LmeA is involved in the distribution of mannoses and glycans in the capsule, or that it stabilizes a protein that serves this function. Further investigation is needed into this theory.

M63 media without tween was able improve Δ*lmeA*'s sensitivity to various antibiotics. WT recovered greatly in the case of vancomycin and erythromycin while Δ*lmeA* recovered less significantly across the different classes of antibiotics. In accordance with all of this antibiotic sensitivity data, Δ*lmeA* is more permeable to ethidium bromide. Taken together, this mutant has a clearly defective cell envelope.

Protein expression in WT and Δ*lmeA* is different, whether in log phase or starvation. In earlier fractions, Δ*lmeA* has increased protein content in starvation lanes relative to any of the other conditions. In later fractions, this trend does not seem to hold true. This is interesting because LmeA is a PMCW protein, localizing to fractions seven through twelve. For this reason, it was surprising to see differences in protein content throughout the different parts of the cell. The four sucrose gradients used for this experiment were made by three different people in the Morita lab. I have re-made all four sucrose gradients in my hands to minimize variability in preparation. These sucrose gradients have yet to be visualized via silver staining, but this will be a next step.

We know that LmeA is a PMCW protein because *in-vivo*, it localizes to PMCW fractions in sucrose gradients. The localization and binding of a protein can give clues to a protein's

function, so fully investigating binding was of interest. LmeA has a signal peptide. This signal peptide can either be cleaved, or it can remain and anchor the protein to the cell envelope; it is unclear which is the case. To investigate, purified LmeA was added to cell lysate, incubated, ran on a sucrose gradient, fractionated, and then ran on a Western blot. Probing for His-LmeA showed that LmeA bound to IMD fractions, or plasma membrane free of cell wall fractions. This indicated that LmeA has no preference for cell wall components. This could lead one to believe that the signal peptide does not get cleaved off, and LmeA remains anchored interacting with the plasma membrane. If the signal peptide got cleaved off, LmeA would be free to float around the periplasm, perhaps having some interaction and thus affinity for the next layer- peptidoglycan.

An experiment that would give us a definitive answer to this question is to visualize LmeA *in*-vivo under the microscope. The issue with this is that LmeA is a small, 29 kDa protein that would not take well to a large fluorescent protein tag. LmeA is periplasmic, so using a tagged LmeA strain to do immunofluorescence would not work. The solution to this is to remove all the layers of the cell envelope from peptidoglycan upwards and to do immunofluorescence with a tagged LmeA strain. We have attempted to do this, successfully forming spheroplasts in the process but we have been unable to produce a reproducible result. If LmeA is anchored to the cell envelope, we should see fluorescence. If LmeA's signal peptide gets chopped off, then LmeA should float away into the media upon the removal of peptidoglycan. This is a future direction that needs to be finished.

One clue that is in agreement with all previous binding data is that LmeA binds spheroplasts. Spheroplasts contain just plasma membrane. LmeA binds spheroplasts both in a sucrose gradient setting and an ELISA setting. It is interesting to note that even in spheroplasts where there is no cell wall, LmeA still migrates to different fractions from our PMCW marker

MptC. It is also interesting to note that based upon this experiment and other experiments done for a different project, IMD proteins seems to disappear upon the formation of a spherical cell. This could branch out to form a small side project- whether or not the IMD is shape dependent. In the ELISA-based spheroplast binding assay, it was interesting to see that LmeA could bind spheroplasts with or without *E. coli* lysate, although binding was better with it. It was also interesting to note that untransformed *E. coli* lysate was used and binding still occurred. Previous data has shown that in order for LmeA to bind to phospholipids, transformed *E. coli* was required.

LmeA has previously been shown to be important for MptA stabilization during stress conditions. Consistent with this data is the above growth recovery curve after starvation. Δ*lmeA* does not have a growth lag when grown in normal conditions. This phenotype is specific to stress. Perhaps the lack of MptA during these conditions leads to a decrease in doubling rate. An experiment to test this would be to see if Δ*mptA* has a growth lag during starvation. If it does and it is similar to the timing of LmeA, this would tell us that this growth lag is an MptA dependent phenomenon. If it does not have a growth lag, it would tell us this phenotype is specific to LmeA. Previous data has shown that an *mptA* knockdown strain does not have a growth lag.

One possibility of LmeA's function is that it is a thioredoxin reductase. This speculation was partially generated based on the fact that LmeA shares an operon with thioredoxin. Genes that share an operon typically operate in the same system. In addition, MptA has conserved cysteine residues that could possibly form disulfide bridges. Perhaps LmeA protects MptA from ThiX-mediated degradation.
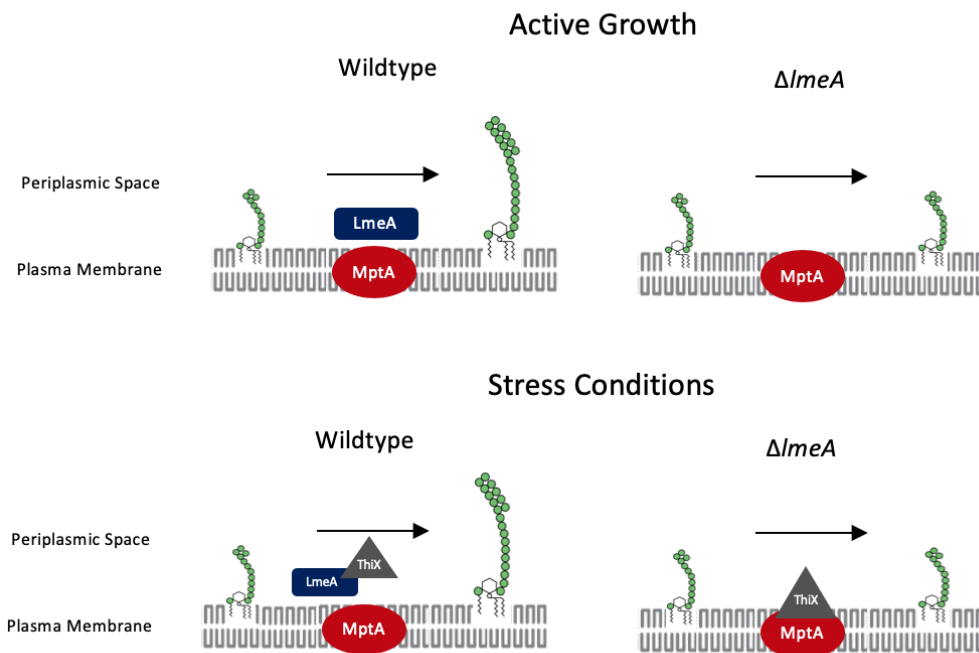
Figure 5.2: Model for LmeA as a Possible Thioredoxin Reductase In this hypothesis, under active growth, LmeA interacts with MptA to produce full length LM/LAM. During stress conditions, LmeA protects MptA from stress-induced-thioredoxin-mediated degradation, allowing for the biosynthesis of mature LM/LAM. In Δ*lmeA*, ThiX degrades MptA, resulting in immature LM/LAM.

A few experiments have to take place for this to above model to be confirmed. First, purified LmeA needs to be tested for thioredoxin reductase activity. Second, purified ThiX needs to be tested for thioredoxin activity. Both proteins have been expressed and purified from *E. coli* expression vectors, so the assay just needs to be done. After this, a next step would be to use the Δ*lmeA*-Δ*thiX* strain made in this study to see if MptA degradation occurs during starvation. If ThiX is responsible for MptA's degradation during starvation in Δ*lmeA*, then no degradation should occur during starvation in this double knockout strain. Another possible step could be to get the crystal structure of MptA to confirm these possible disulfide bridges. MptA currently does not have crystal structure due to the fact that it is a membrane protein, which are infamous for being

48

difficult to accurately crystallize. Preliminary data may support this hypothesis. An easier way to test for disulfide bridges would be to use a commercially available fluorescent dye that binds to disulfide bonds. A previous student performed thiol trapping on MptA in the Δ*lmeA* strain and showed that MptA contained no disulfide bonds relative to WT. This experiment needs to be repeated with additional control, such as using the Δ*thiX* strain to see if the phenotype is the same, confirming our hypothesis. Another experiment would be to perform thiol trapping on the Δ*lmeA*-Δ*thiX* strain to see if these disulfide bonds remain absent in MptA.

Another interesting future direction would be to use the *lmeA-HA-ΔthiX* strain to see if LmeA localization changes in the absence of ThiX. Perhaps LmeA's sole function is to protect MptA from degradation and if ThiX is not present, LmeA could be downregulated or its localization could change. mRNA transcripts of *lmeA* for this strain could be done to check for *lmeA* levels as well as a sucrose gradient to check for changes in localization. Looking back at Figure 5.1, Δ*lmeA* has fewer insertions in *MSMEG_5470c* which encodes for molybdopterin biosynthesis protein MoeA 1. This protein is involved in redox reactions, as is ThiX. Literature has shown that ThiX has physical interactions with MoeA in other organisms such as *E. coli*, and programs like string tie together thioredoxins with redox proteins related to MoeA.

There are many clues to LmeA's exact function but still no smoking gun. With the purified ThiX and the knockout strain that were made, LmeA's role in cell envelope biosynthesis could be determined soon.

Chapter 6
Methods

6.1 Bacterial Strains and Growth Conditions

Wild-type (WT) *M. smegmatis* mc$_2$155 (Snapper *et al.*1990), Δ*pimE*, Δ*pimE::pimE*[41] , Δ*lmeA*, Δ*lmeA::*Pnative-LmeA-HA, Δ*lmeA::*Phsp60-LmeA-HA[35] were grown in 130 rpm planktonic conditions at 30°C or 37°C in a liquid culture of Middlebrook 7H9 manufactured by Becton Dickinson. 7H9 was supplemented with 0.2% glycerol, 0.2% glucose, 15 mM NaCl, and 0.05% tween. Other cultures were grown in M63 minimal media, of which the recipe can be found in Eagen et al. 2018[34] . Culture was grown to log phase (OD600 0.6-1). For starvation conditions, once log phase was reached, the cultures were spun down at 4000 rpm for 5 minutes, washed with sterile phosphate-buffered saline, spun down as described before, resuspended in the original volume in sterile phosphate-buffered saline, and starved for 24 hours. For the recovery assay, cultures in PBS were spun down as described above and resuspended in 7H9 complete media, as described above and OD600 was monitored.

6.2 Antibiotic Sensitivity Assay

Frozen stocks with known colony forming units (cfu) were prepared for all tested strains by growing cells to an OD$_{600}$ reading between 0.5 and 1.0 in Middlebrook 7H9 or M63, and frozen in aliquots with a final concentration of 15% (w/v) glycerol at –80°C. In 96-well microtiter plates, antibiotics were serially diluted in 100 μl of media and mixed with cells from the frozen stocks to achieve the final density of $5.0 \times 10_3$ cfu/mL. The plates were incubated in a humidity chamber either at 30 °C or 37°C. After a 24 hour 32 hour incubatiom, 20 μL of filter-sterilized 0.015% (w/v) resazurin solution was added to each well to initiate colorization. After

additional 8 hour (37°C) or 13.5 hour (30°C) incubation, the plates were read on a spectrophotometer at 570 and 600 nm. Percent difference in cell viability between antibiotic-treated and control cells was calculated using the formula: $(O2 \times A1 - O1 \times A2)/(O2 \times P1 - O1 \times P2) \times 100$, where O1 and O2 are molar extinction coefficient of resazurin (oxidized form) at 570 and 600 nm, respectively; A1 and A2 are absorbance of test wells at 570 and 600 nm, respectively; and P1 and P2 are absorbance of positive control well at 570 and 600 nm, respectively. The IC_{90} values were calculated using OriginPro 9.1 data analysis software.

6.3 Ethidium Bromide Uptake Assay

Ethidium bromide uptake assay was done in accordance to Eagen et. Al, 2018[34]. Briefly, log phase ($OD_{600} = 0.5–1.0$) cells grown in 7H9 were centrifuged and pellets were resuspended at an equal OD_{600} reading in 50 mM KH_2PO_4 (pH 7.0) and 5 mM $MgSO_4$. Cells were then incubated for 5 min with 25 mM glucose, transferred to an opaque, black 96-well microtiter plate (Brand Tech Scientific), and mixed with 20 µM of ethidium bromide. Fluorescence was measured with an excitation wavelength of 530 nm and an emission wavelength of 590 nm.

6.4 Capsule Staining

20 mL primary cultures were inoculated into Middlebrook 7H9 supplemented with 0.2% glycerol, 0.2% glucose, 15 mM NaCl, *without* tween and grown at 37°C. After 3-4 days, secondary cultures were inoculated, also without tween. After 16-18 hours, cells were pelleted at 4000 rpm for 5 minutes and resuspended in 450 µL of PBS and 50 µl of 2 mg/ml of FITC-fluorescent-conjugated lectin Concanavalin A suspended in 0.1M sodium bicarbonate and incubated for 30 minutes at 37°C. The solution was spun down at 12000 rpm for three minutes, washed with PBS, and spun again. The final pellet was suspended in resuspended in 100 µl PBS.

5-10 µl of this solution was pipetted onto a 1% agarose in 7H9 gel pad atop a glass slide and visualized via fluorescent microscopy.

6.5 Silver Staining

A BCA assay was first done to determine protein content per sucrose gradient fraction. 10 µL of each sample was added to a 96 well plate. 200 µL of the Pierce BCA Protein Assay Kit was added to each well and incubated in the dark for 30 minutes at 37°C. The plate was then read in a spectrophotometer at 562 nm. These values were then used to standardize protein content before silver staining. 12 µL of each sucrose gradient fraction standardized for protein content was mixed with 4 µL of loading buffer and boiled at 95°C for five minutes. Each sample was then loaded onto a 12% acrylamide SDS-PAGE gel and ran at 150V. The gel was incubated with a fixative solution for 45 minutes and washed three times with Milli-Q water. The gel was then incubated a sensitizing solution for 2 minutes and washed with water for 5 minutes. The gel was then incubated with a silvering solution fo r45 minutes and rinsed for 20 second with water afterwards. A developer solution was added for 6-8 minutes until the stop solution was added to stop the reaction.

6.6 LmeA Purification

Protocol by Kathryn Rahlwes. *E. coli* BL21 cells transfected with pMUM 121 was inoculated into 20 mL TBK with 100 µg/ml ampicillin and grown at 37°C overnight. 5 mL was inoculated into 500 mL TBK and incubated at 30°C planktonically at 130 rpm until OD600 reached 0.6. A final concentration of 1 mM IPTG was added.

After 3 hours of incubation with IPTG, the culture was spun down at 8000 rpm for 10 min at 4°C. Supernatant was discarded and pellet was resuspended in 40 mL PBS and transferred

to a 50 mL conical tube. Weight of pellet was measured. Add 1 mL of lysis buffer (see recipe below) per 0.25 g pellet. Incubate 10 min at room temperature. Sonicate on ice for 10 sec and repeat five times, keeping on ice in between sonications. Transfer sonicated sample to 15 mL conical tube and centrifuge for 30 min at 4°C. Transfer supernatant and spin again. Filter supernatant though 0.22 µM syringe filter to remove any remaining cell debris.

LmeA was purified from an *E. coli* IPTG inducible expression vector using a nickel affinity column. LmeA purification materials used include Ni NTA Resin (GoldBio, H-250-25), 20 mM HEPES pH 7.5, Amicon Ultra-4, Lysis buffer (3.9 mL of 50 mM HEPES pH 7.5, 200 mM NaCl, 50 µL 100 mM PMSF in 50 mM HEPES pH 7.5, 50 µl 100 mM DTT, 500 µL 10 mg/ml Lysozyme), wash buffer (100 mM HEPES pH 7.5, 10 mM imidazole, 500 mM NaCl), elution buffer 1 (100 mM HEPES pH 7.5, 75 mM imidazole, and elution buffer 2 (100 mM HEPES pH 7.5, 125 mM imidazole), elution buffer 3 (100 mM HEPES pH 7.5, 250 mM imidazole). 250 µl of bed volume of Ni NTA Resin was loaded onto a 15 ml column and washed with 5 volumes of wash buffer. 10 mL of lysate was incubated in this overnight at 4°C while rotating. The next day, the column was opened and the flow through was collected. Wash the resin with 1 mL of wash buffer plus 0.05% tween. Wash three times with wash buffer without tween. Elute penta-His-tagged-LmeA using 200 µL elution buffer 1, then elution buffer 2, then elution buffer 3. Repeat until 15 fractions are collected. Run all samples on SDS-PAGE and visualize with Coomassie Brilliant Blue. Fractions containing peak His-LmeA are combined, concentrated, washed three times with 20 µM HEPES pH 7.5, and resuspended in a final volume of 1 mL containing 20% glycerol.

6.7 *In-vitro* and *In*-vivo Sucrose Gradient Fractionation

2.5 mL of primary cultures were inoculated into three 500 mL cultures containing 7H9 complete. After 16-18 hours of planktonic growth at 37°C, or until the OD600 reaches 0.6-1. These cultures were then spun down at 8000 rpm for 15 minutes at 4°C. The supernatant was poured off and the pellets were resuspended in 50 mM Hepes/NaOH (pH 7.4), spun again as above, and resuspended in 5 ml of lysis buffer per 1 gram of wet pellet. Lysis buffer: 25 mM Hepes (pH7.4), 20% sucrose in 25 mM Hepes, 2 mM EGTA. 1/25 volume lysis buffer of protease inhibitor was added. 2200 psi of nitrogen gas for thirty minutes was applied to this mixture three times to lyse cells. The lysed cell mixture was centrifuged for 4000 rpm for 10 min at 4°C. The supernatant was removed and centrifuged as before. 1200 µL of this solution was placed atop a 20-50% sucrose gradient and centrifuged at 35000 rpm for 6 hours at 4°C. For the *in-vitro* experiment, 1 mg/mL of purified protein was added and incubated at 37°C for 30 minutes before loading onto the sucrose gradient. The gradient was then fractionated into 13 fractions and stored at 80°C.

6.8 ELISA Spheroplast Binding Assay

Either spheroplasts or isopropanol were added to the bottom of an ELISA plate. The plate was evaporated without the lid at 37°C for 2 hours. 20 µL of hexanes was added to all wells to block and evaporated in a fume hood for 20 minutes. 5% milk was then added for 16-19 hours at 4°C without shaking with the cover. The wells were washed twice for five minutes with 200 µL of PBST. 10 µL of 1 mg/mL protein was added to each well and incubated for two hours at 37°C. The wells were washed with 200 µL PBST for 5 minutes at room temperature three times. 50 µL of 1:4000 penta-his primary antibody was added to each well and incubated for one hour

at room temperature. Each well was washed with 200 µL PBST for five minutes three times. 100 µL of TMB colorization reagent was added to each well and incubated for one hour at room temperature in the dark. The plate was then read at 650 nm.

6.9 Post-Starvation Growth Recovery Curve

WT and Δ*lmeA* were inoculated into 20 mL cultures containing Middlebrook 7H9 supplemented with 0.2% glycerol, 0.2% glucose, 15 mM NaCl, and 0.05% tween and grown for 3-4 days planktonically at 37°C. Secondary cultures were then innoculated and grown for 16-18 hours or until an OD600 of 0.6-1.0 was reached. The cultures were were spun down at 4000 rpm for 5 minutes, washed with sterile phosphate-buffered saline, spun down as described before, resuspended in the original volume in sterile phosphate-buffered saline, and starved for 24 hours. For the recovery assay, cultures in PBS were spun down as described above and resuspended in 7H9 complete media, as described above and OD600 was monitored.

6.10 Making Spheroplasts

A secondary culture of *M. smegmatis* was grown at 37°C until an OD600 of 0.6-1 was reached. Glycine was added to the culture to a final concentration of 1.2% (w/v) and incubated for another 20-24 hours. The culture was then centrifuged at 4000 rpm for 5 minutes and washed with Spizizen's minimal medium (SMM), spun again above, and resuspended in SMM at the original volume of the culture. A filter sterilized solution of 5 mg/ml lysozyme at 20% w/v and glycine at 1.2% w/v was added. The culture was incubated for another 20-24 hours. The formation of spheroplasts was confirmed by microscopy.

6.11 Polymerase Chain Reaction (PCR) Amplification

For PCR amplification to generate inserts for ligation, each tube contained the following: 12.8 µl of Pre-Mix (8.8 µL water per tube, 3.2 µl 5x Phusion HF buffer per tube, 0.4 µl 10 mM dNTPs per tube, 0.4 µl 0.1 ng/µl genomic DNA per tube), 1 µL each of forward/reverse primer, 0.8 µL DMSO, and 0.4 µL water. After heating to 98°C, 4 µL of hot start mix was added to each tube (3 µL water per tube, 0.8 µL 5x Phusion HF buffer per tube, 0.2 µL Phusion DNA Polymerase per tube). The reaction continued thirty times. The resulting DNA was run on a 1% agarose gel and visualized via ethidium bromide incubation and UV light.

For PCR amplification to confirm extracted *M. smeg* genomic DNA, the above concentrations were used with an added 4 µL of extracted DNA. DNA was extracted by incubating frozen stock for 30 minutes on a 95°C heating block. The sample was micro centrifuged at 16000 rpm for 2 minutes and the supernatant was transferred to a new tube. 200 µl of 24:1 (w/v) chloroform/isoamyl alchol mix was added to the sample and briefly vortexed to extract proteins and lipids. The sample was placed on ice and 1/10 volume of 3M sodium acetate and 2.5 volumes of ice-cold 100% ethanol was added. The sample was micro centrifuged for 5 minutes at 4°C, the supernatant was poured off, and and the pellet was air-dried until all ethanol was evaporated. The pellet was resuspended in 100 µL milliQ water.

PCR clean-up was done with a Qiagen QIAquick Gel Extraction kit. 5 volumes of Buffer PB was added to the sample and 3M Na-Acetate (pH 5.0) was added until sample turned yellow. Sample was applied onto a QIAquick column and spun for 1 minute and repeated. The column was washed with 750 µL Buffer PE and incubated for 2-5 minutes before spinning. The column was transferred to a new tube and the DNA was eluted with pre-warmed (60°C) Buffer EB that was incubated for 5 minutes at room temperature before spinning.

6.12 HiFi Assembly

First the DNA concentrations of digested vector and inserts were measured using Nanodrop. For DNA ranging from 0.03-0.2 pmol, the ratio of vector to insert was 1:2. The following equation was used for calculations: pmols = (weight in ng) x 1000 / (base pairs x 650 daltons). After calculating and mixing the proper ratio of vector to insert, 1 volume of NEBuilder Master Mix was added and the sample was incubated for 15 minutes at 50°C. 5 µl of this plasmid was added to 250 µL of *E. coli* lab-made competent cells and placed on ice for 30 minutes. Then the cells were heat shocked at exactly 42°C in.a water bath for 45 seconds. The sample was placed on ice for 2 minutes and 950 µL of room temperature SOC broth was added to each tube. The sample was incubated for 60 minutes at 37°C. 100 µL of this mixture was pipetted onto selection plates containing the proper antibiotic and incubated overnight at 37°C. Colonies were picked and grown in 2 ml of TBK media with proper antibiotic overnight. The cells were pelleted and the supernatant was poured off. The pellet was resuspended in ice-cold 200 µL Qiagen Buffer P1. 200 µL of Buffer P2 and P3 were added to the sample and inverted to mix. 50 µl chloroform was added and vortexed. The sample was spun down at 4°C and the upper phase was transferred to a new tube. 1/10 volume 3M Na-acetate (pH 5.2) was added and DNA was precipitated by adding 2 volumes of ice-cold ethanol and inverted to mix. Plasmid DNA was collected by spinning at max speed at 4°C for 10 minutes and the supernatant was removed. 1 mL of ice-cold 70% ethanol was added to the pellet and the tube was inverted. The sample was spun down at max speed for 2 minutes at 4°C and the supernatant was removed thoroughly using an aspirator. The pellet was air dried until the pellet looked translucent. The pellet was resuspended in Buffer EB. The plasmid DNA was then used for restriction enzyme digestion and candidate plasmids were sent for Sanger sequencing.

BIBLIOGRAPHY

1. Gerszten PC, Gerszten E, Allison MJ. Diseases of the spine in south american mummies. *Neurosurgery*. 2001;48(1):208-213. https://academic.oup.com/neurosurgery/article/48/1/208/2748891. Accessed Apr 3, 2020. doi: 10.1097/00006123-200101000-00039.

2. Cave AJE, Demonstrator A. The evidence for the incidence of tuberculosis in ancient egypt. *British Journal of Tuberculosis*. 1939;33(3):142-152. http://www.sciencedirect.com/science/article/pii/S0366085039800163. Accessed Apr 3, 2020. doi: 10.1016/S0366-0850(39)80016-3.

3. History | world TB day | TB | CDC. https://www.cdc.gov/tb/worldtbday/history.htm. Updated 2019. Accessed Apr 3, 2020.

4. Tuberculosis. https://www.who.int/westernpacific/health-topics/tuberculosis. Accessed Apr 3, 2020.

5. Data & statistics | TB | CDC. https://www.cdc.gov/tb/statistics/default.htm. Updated 2020. Accessed Apr 3, 2020.

6. Information, National Center for Biotechnology, Pike, U. S. National Library of Medicine 8600 Rockville, MD B, Usa 2. *Treatment of tuberculosis patients.* World Health Organization; 2008. https://www.ncbi.nlm.nih.gov/books/NBK310759/. Accessed Apr 3, 2020.

7. Mahajan R. Bedaquiline: First FDA-approved tuberculosis drug in 40 years. *Int J Appl Basic Med Res*. 2013;3(1):1-2. https://www.ncbi.nlm.nih.gov/pmc/articles/PMC3678673/. Accessed Apr 3, 2020. doi: 10.4103/2229-516X.112228.

8. Lange C, Chesov D, Heyckendorf J, Leung CC, Udwadia Z, Dheda K. Drug-resistant tuberculosis: An update on disease burden, diagnosis and treatment. *Respirology*. 2018;23(7):656-673. Accessed Apr 3, 2020. doi: 10.1111/resp.13304.

9. Das S, Bhattacharjee O, Goswami A, Pal NK, Majumdar S. Arabinosylated lipoarabinomannan (ara-LAM) mediated intracellular mechanisms against tuberculosis infection: Involvement of protein kinase C (PKC) mediated signaling. *Tuberculosis (Edinb)*. 2015;95(2):208-216. Accessed Apr 3, 2020. doi: 10.1016/j.tube.2014.11.007.

10. Hayashi JM, Luo C, Mayfield JA, et al. Spatially distinct and metabolically active membrane domain in mycobacteria. *PNAS*. 2016;113(19):5400-5405. Accessed Apr 3, 2020.

11. Hayashi JM, Richardson K, Melzer ES, et al. Stress-induced reorganization of the mycobacterial membrane domain. *mBio*. 2018;9(1). Accessed Apr 3, 2020. doi: 10.1128/mBio.01823-17.

12. Zuber B, Chami M, Houssin C, Dubochet J, Griffiths G, Daffé M. Direct visualization of the outer membrane of mycobacteria and corynebacteria in their native state. *J Bacteriol*. 2008;190(16):5672-5680. Accessed Apr 3, 2020. doi: 10.1128/JB.01919-07.

13. Ito T, Hasegawa A, Hosokawa H, et al. Human Th1 differentiation induced by lipoarabinomannan/lipomannan from mycobacterium bovis BCG tokyo-172. *Int Immunol*.

2008;20(7):849-860. https://academic.oup.com/intimm/article/20/7/849/694637. Accessed Apr 22, 2020. doi: 10.1093/intimm/dxn043.

14. Bansal-Mutalik R, Nikaido H. Mycobacterial outer membrane is a lipid bilayer and the inner membrane is unusually rich in diacyl phosphatidylinositol dimannosides. *PNAS*. 2014;111(13):4958-4963. Accessed Apr 3, 2020.

15. Kalscheuer R, Palacios A, Anso I, et al. The mycobacterium tuberculosis capsule: A cell structure with key implications in pathogenesis. *Biochem J*. 2019;476(14):1995-2016. https://www.ncbi.nlm.nih.gov/pmc/articles/PMC6698057/. Accessed Apr 16, 2020. doi: 10.1042/BCJ20190324.

16. Hansmeier N, Albersmeier A, Tauch A, et al. The surface (S)-layer gene cspB of corynebacterium glutamicum is transcriptionally activated by a LuxR-type regulator and located on a 6 kb genomic island absent from the type strain ATCC 13032. *Microbiology (Reading, Engl)*. 2006;152(Pt 4):923-935. Accessed Apr 3, 2020. doi: 10.1099/mic.0.28673-0.

17. Hoischen C, Gura K, Luge C, Gumpert J. Lipid and fatty acid composition of cytoplasmic membranes from streptomyces hygroscopicus and its stable protoplast-type L form. *J Bacteriol*. 1997;179(11):3430-3436. https://www.ncbi.nlm.nih.gov/pmc/articles/PMC179132/. Accessed Apr 3, 2020.

18. Howlett R, Anttonen K, Read N, Smith MCM. Disruption of the GDP-mannose synthesis pathway in streptomyces coelicolor results in antibiotic hyper-susceptible phenotypes. *Microbiology (Reading, Engl)*. 2018;164(4):614-624. Accessed Apr 3, 2020. doi: 10.1099/mic.0.000636.

19. Kovacevic S, Anderson D, Morita YS, et al. Identification of a novel protein with a role in lipoarabinomannan biosynthesis in mycobacteria. *J Biol Chem*. 2006;281(14):9011-9017. http://www.jbc.org/content/281/14/9011. Accessed Apr 3, 2020. doi: 10.1074/jbc.M511709200.

20. Morita YS, Sena CBC, Waller RF, et al. PimE is a polyprenol-phosphate-mannose-dependent mannosyltransferase that transfers the fifth mannose of phosphatidylinositol mannoside in mycobacteria. *J Biol Chem*. 2006;281(35):25143-25155. Accessed Apr 3, 2020. doi: 10.1074/jbc.M604214200.

21. Rainczuk AK, Yamaryo-Botte Y, Brammananth R, et al. The lipoprotein LpqW is essential for the mannosylation of periplasmic glycolipids in corynebacteria. *J Biol Chem*. 2012;287(51):42726-42738. http://www.jbc.org/content/287/51/42726. Accessed Apr 3, 2020. doi: 10.1074/jbc.M112.373415.

22. Mishra AK, Alderwick LJ, Rittmann D, et al. Identification of an alpha(1-->6) mannopyranosyltransferase (MptA), involved in corynebacterium glutamicum lipomanann biosynthesis, and identification of its orthologue in mycobacterium tuberculosis. *Mol Microbiol*. 2007;65(6):1503-1517. Accessed Apr 3, 2020. doi: 10.1111/j.1365-2958.2007.05884.x.

23. Mishra AK, Krumbach K, Rittmann D, et al. Lipoarabinomannan biosynthesis in corynebacterineae: The interplay of two α(1→2)-mannopyranosyltransferases MptC and MptD in mannan branching. *Mol Microbiol*. 2011;80(5):1241-1259. Accessed Apr 3, 2020. doi: 10.1111/j.1365-2958.2011.07640.x.

24. Korkegian A, Roberts DM, Blair R, Parish T. Mutations in the essential arabinosyltransferase EmbC lead to alterations in mycobacterium tuberculosis lipoarabinomannan. *J Biol Chem*. 2014;289(51):35172-35181. Accessed Apr 3, 2020. doi: 10.1074/jbc.M114.583112.

25. Zhang J, Amin AG, Hölemann A, Seeberger PH, Chatterjee D. Development of a plate-based scintillation proximity assay for the mycobacterial AftB enzyme involved in cell wall arabinan biosynthesis. *Bioorg Med Chem*. 2010;18(19):7121-7131. Accessed Apr 3, 2020. doi: 10.1016/j.bmc.2010.07.040.

26. Zhang J, Angala SK, Pramanik PK, et al. Reconstitution of functional mycobacterial arabinosyltransferase AftC proteoliposome and assessment of decaprenylphosphorylarabinose analogues as arabinofuranosyl donors. *ACS Chem Biol*. 2011;6(8):819-828. Accessed Apr 3, 2020. doi: 10.1021/cb200091m.

27. C. Rahlwes K. *Regulation of lipomannan and lipoarabinomannan in mycobacteria.* University of Massachusetts Amhrest; 2018.

28. Hammes W, Schleifer KH, Kandler O. Mode of action of glycine on the biosynthesis of peptidoglycan. *J Bacteriol*. 1973;116(2):1029-1053.
https://www.ncbi.nlm.nih.gov/pmc/articles/PMC285483/. Accessed Apr 3, 2020.

29. Mukherjee R, Chatterji D. Glycopeptidolipids: Immuno-modulators in greasy mycobacterial cell envelope. *IUBMB Life*. 2012;64(3):215-225.
https://iubmb.onlinelibrary.wiley.com/doi/abs/10.1002/iub.602. Accessed Apr 23, 2020. doi: 10.1002/iub.602.

30. Miyoshi-Akiyama T, Matsumura K, Iwai H, Funatogawa K, Kirikae T. Complete annotated genome sequence of mycobacterium tuberculosis erdman. *J Bacteriol*. 2012;194(10):2770. Accessed Apr 3, 2020. doi: 10.1128/JB.00353-12.

31. Stinear TP, Seemann T, Harrison PF, et al. Insights from the complete genome sequence of mycobacterium marinum on the evolution of mycobacterium tuberculosis. *Genome research*. 2008;18(5):729-741. https://www.ncbi.nlm.nih.gov/pubmed/18403782. doi: 10.1101/gr.075069.107.

32. Goude R, Amin AG, Chatterjee D, Parish T. The arabinosyltransferase EmbC is inhibited by ethambutol in mycobacterium tuberculosis. *Antimicrob Agents Chemother*. 2009;53(10):4138-4146. Accessed Apr 3, 2020. doi: 10.1128/AAC.00162-09.

33. Timmins GS, Deretic V. Mechanisms of action of isoniazid. *Mol Microbiol*. 2006;62(5):1220-1227. Accessed Apr 3, 2020. doi: 10.1111/j.1365-2958.2006.05467.x.

34. Eagen WJ, Baumoel LR, Osman SH, Rahlwes KC, Morita YS. Deletion of PimE mannosyltransferase results in increased copper sensitivity in mycobacterium smegmatis. *FEMS Microbiol Lett*. 2018;365(6). https://academic.oup.com/femsle/article/365/6/fny025/4830098. Accessed Apr 3, 2020. doi: 10.1093/femsle/fny025.

35. Rahlwes KC, Ha SA, Motooka D, et al. The cell envelope–associated phospholipid-binding protein LmeA is required for mannan polymerization in mycobacteria. Journal of Biological Chemistry Web site. http://www.jbc.org. Accessed Apr 3, 2020.

36. Perkowski EF, Zulauf KE, Weerakoon D, et al. The EXIT strategy: An approach for identifying bacterial proteins exported during host infection. *mBio*. 2017;8(2). Accessed Apr 22, 2020. doi: 10.1128/mBio.00333-17.

37. Fukuda T, Matsumura T, Ato M, et al. Critical roles for lipomannan and lipoarabinomannan in cell wall integrity of mycobacteria and pathogenesis of tuberculosis. *mBio*. 2013;4(1):472. Accessed Apr 3, 2020. doi: 10.1128/mBio.00472-12.

38. Watanakunakorn C. Mode of action and in-vitro activity of vancomycin. *J Antimicrob Chemother*. 1984;14 Suppl D:7-18. Accessed Apr 3, 2020. doi: 10.1093/jac/14.suppl_d.7.

39. Williamson R, Collatz E, Gutmann L. [Mechanisms of action of beta-lactam antibiotics and mechanisms of non-enzymatic resistance]. *Presse Med*. 1986;15(46):2282-2289. Accessed Apr 3, 2020.

40. Gaynor M, Mankin AS. Macrolide antibiotics: Binding site, mechanism of action, resistance. *Curr Top Med Chem*. 2003;3(9):949-961. Accessed Apr 3, 2020. doi: 10.2174/1568026033452159.

41. Morita YS, Sena CBC, Waller RF, et al. PimE is a polyprenol-phosphate-mannose-dependent mannosyltransferase that transfers the fifth mannose of phosphatidylinositol mannoside in mycobacteria. *J Biol Chem*. 2006;281(35):25143-25155. Accessed Apr 3, 2020. doi: 10.1074/jbc.M604214200.